EXPLOITING SPECTRUM AGILITY IN WIRELESS LINKS AND NETWORKS

Approved by:

Dr. Joseph Camp

Dr. Dinesh Rajan

Dr. Eli Olinick

Dr. Carlos Davila

Dr. Panos Papamichalis

EXPLOITING SPECTRUM AGILITY IN WIRELESS LINKS AND NETWORKS

A Dissertation Presented to the Graduate Faculty of the

Bobby B. Lyle School of Engineering

Southern Methodist University

in

Partial Fulfillment of the Requirements

for the degree of

Doctor of Philosophy

with a

Major in Electrical Engineering

by

Pengfei Cui

(B.S., Beijing Institute of Technology, 2007)
(M.S., University of Chinese Academy of Sciences, 2010)

TBA

ACKNOWLEDGMENTS

One of the great joys of completion is to look over the journey past and remember all the friends and family who have helped and supported me along this long but fulfilling road.

First and formost, I would like to thank my advisor, Dr. Joseph Camp, who provided seemingly endless resources to support my work. I would also like to thank my co-advisor, Dr. Dinesh Rajan, who always provides great comments and suggestions on my research, presentations and publications. They are not only my academic mentors but also model examples of 'American Dream' I can touch. I could not have asked for better role models, each inspirational, supportive, and patient. I would not be where I am today without the time and effort you spent throughout my studies. Thanks also go to my other committee member, Dr. Panos Papamichalis, Dr. Carlos Davila, Dr. Eli Olinick, for providing novel perspectives to my work.

Special thanks to Dr. Joseph Cleveland, who offered several courses and always joined in our group discussion. Thanks to Buses By Bill Inc. and Bill Austin for their supports of our measurements system.

I am thankful for the collaborations and discussions within our research group, including Yongjiu Du, Jonathan Landon, Pengda Huang, Hui Liu, Jialin He, Matthew Tonnemacher, Eric Johnson, Yingsi Liang, Rita Enami, Bryan Jeon and Tiaotiao Wang. I am thinkful for collaboration with Jialin He, Hui Liu, Jonathan Landon, Dr. Onur Altintas, Rama Vuyyuru, Yuanyuan Dong, Dr. Eli Olinick, Dr. Ehsan Aryafa, and Dr. Mung Chiang.

I would like to thank my friends, Yu Gan, Fujun Liu, Jinyang Liang, Junjie Ma, Ting Li, Wei Liu and Dr. Silin Wang for their help and encouraging for my Ph.D

studies.

I would like to express my heartfelt gratitude to my wife, Yulin Wang. Without her love, support, patience and help, I would not overcome the hard times throughout my Ph.D studies.

I am indebted to my family, especially to my mother and father, for believing in me to complete this work.

Last, but not least, thanks to all people participate in our experiments.

Cui , Pengfei B.S., Beijing Institute of Technology, 2007
M.S., University of Chinese Academy of Sciences, 2010

Exploiting Spectrum Agility in Wireless Links and Networks

Advisor: Professor Joseph Camp

Doctor of Philosophy degree conferred TBA

Dissertation completed TBA

In 2009, the FCC approved the use of broadband services in the white space frequency of UHF TV bands, which were formerly exclusively licensed to television broadcasters. Here, bands represent the continuous frequency have same or similar propagation characteristics, for instance 2.4 GHz band, 5 GHz band; channel notes a piece of frequency directly used for communication with a small bandwidth, such as 20 MHz. These white space bands are now available for unlicensed public use, offering new opportunities for the design of devices and networks with better performance in terms of throughput and cost. People are working to implement the new opportunities in the field to serve people better. In this thesis, we seek to exploit these new spectrum opportunities in wireless links and networks. In particular, while many metropolitan areas sought to deploy city-wide WiFi networks, the densest urban areas were not able to broadly leverage the technology for large-scale Internet access. Ultimately, the small spatial separation required for effective 802.11 links in these areas resulted in prohibitively large up-front costs. The far greater range of these lower white space carrier frequencies are especially critical in rural areas, where high levels of aggregation could dramatically lower the cost of deployment and is in direct contrast to dense urban areas in which networks are built to maximize spatial reuse. Though both academic and industry experts are eagerly looking forward to the application of these white space bands, more solid theoretic and practical work need to be done of this topic. Here to enable efficient real-world deployments, we investigate spectrum agility in both link communication and network deployment to answer part of the

questions.

First, wireless frequency bands is the foundation and one of the key parts of further wireless applications. We build a measurement driven algorithm to discover the best channel in a vehicular multiband environment. We leverage knowledge of in-situ operation across frequency bands with real-time measurements of the activity level to select the the band with the highest throughput. To do so, we perform a number of experiments in typical vehicular topologies. With two models based on machine learning algorithms and an in-situ training set, we predict the throughput based on: (*i.*) prior performance for similar context information (*e.g.*, SNR, GPS, relative speed, and link distance), and (*ii.*) real-time activity level and relative channel quality per band. In the field, we show that training on a repeatable route with these machine learning techniques can yield vast performance improvements from prior schemes. Second, leveraging a broad range of spectrum across diverse population densities becomes a critical issue for the deployment of data networks with WiFi and white space bands. To address this issue we propose a measurement-driven band selection framework, Multiband Access Point Estimation (MAPE). Then we apply the framework with the data measured the spectrum utility in the Dallas-Fort Worth metropolitan and surrounding areas to show the white space band benefit in network deployment. In particular, we study the white space and WiFi bands with in-field spectrum utility measurements, revealing the number of access points required for an area with channels in multiple bands. In doing so, we find that networks with white space bands reduce the number of access points by up to 1650% in sparse rural areas over similar WiFi-only solutions. In more populated rural areas and sparse urban areas, we find an access point reduction of 660% and 412%, respectively. However, due to the heavy use of white space bands in dense urban areas, the cost reductions invert (an increase in required access points of 6%). Finally, we numerically analyze

band combinations in typical rural and urban areas and show the critical factor that leads to cost reduction: considering the same total number of channels, as more channels are available in the white space bands, less access points are required for a given area.

Furthermore, we compare the heterogeneous access points with simultaneous access to multiple frequency bands in a variety configurations to discover the best set of spectrum combinations for an access point. In particular, we address a heterogeneous white space and WiFi access tier deployment problem and propose a relaxed ILP to get the lower bound of the amount of access point under resource limitations and a heuristic approach to the problem. Then, we map the problem as a bin packing problem and propose to Multiband Heterogeneous Access Point Deployment (MHAPD) method to address the problem. In doing so, we discuss the benefit of white space bands in reducing the number of access points and provide a heuristic solution for wireless network deployment. The numeric results shows that MHAPD gains 260% against the linear hexagon deployment method. We further analyze the performance of heterogeneous access point performance in a variety of population densities. The numeric results show that heterogeneous multiband access points could improve the budget saving upto 323%.

Moreover, the white spaces resource distribution is restricted by FCC contrast to the population density, dense area has few white space channels. Thus, leveraging the range of spectrum across user mobility becomes a critical issue for the operating of heterogeneous data networks with WiFi and limited white space bands. We present a feasibility analysis for a heterogeneous network resource allocation to reduce the power consumption via queuing theory approach. In particular, we study the spectrum utility across multi-bands and the user mobility across a weekday in typical environment of the Dallas-Fort Worth metroplex through measurements. Moreover,

we propose a Greedy Server-side Replace (GSR) algorithm to reduce the power consumption with white space channels application. In doing so, we find that networks with white space bands reduce the power consumption by up to 512.55% in sparse rural area over WiFi-only solutions via measurements driven numerical simulation. In more populated areas. we find an power consumption reduction on average across 24 hours by 24.57%, 46.27%,67.40% over WiFi only network with one to three white space channels respectively. We further investigate the quality of service requirements impacts on power consumption across the number of channels. We find that the power consumption reduction is up to 150.89% with three white space channels in dense areas with relaxed required waiting time.

Then, to quantify the spectrum utilization and far greater range of lower carrier frequencies on multihop access networks, we present an integer linear programming model to leverage diverse propagation characteristics and the channel occupancy of white space and WiFi bands to deploy optimal wireless multiband networks. Since such problem is known to be NP-hard, we design a measurement driven heuristic algorithm, Band-based Path Selection (BPS), which we show approaches the performance of the optimal solution with reduced complexity. We additionally compare the performance of BPS against two well-known multi-channel, multi-radio deployment algorithms across a range of scenarios spanning those typical for rural areas to urban areas. In doing so, we achieve up to 160% of these traffic achieved at gateways versus these existing multi-channel, multi-radio algorithms, which are agnostic to diverse propagation characteristics across bands. Moreover, we show that, with similar channel resources and bandwidth, the joint use of WiFi and white space bands can achieve a served user demand of 170% that of mesh networks with only WiFi bands or white space bands, respectively. Further, through the result, we leverage the channel occupancy and spacing impacts on mesh networks which use white space bands and

study the general rules for band selection.

TABLE OF CONTENTS

LIST OF FIGURES

LIST OF TABLES

Chapter 1

Introduction

Due to the ubiquity and convenience of wireless Internet service, the demand of wireless device users for efficient wireless links and networks are surging. For example, wireless data traffic has increased for a thousand-fold over the last years and is expected to continue over the next decade [1], greatly motivating the improvement of wireless link communication and network deployment technology.

However, unlike wired networks, wireless devices share spectrum resources and have unstable, time-varying channel quality. For a vehicular environment, the situation is even worse due to the frequently changing channel state. Drivers and passengers around the world could utilize a wide array of vehicular applications ranging from real-time traffic monitoring and safety applications to various infotainment applications. However, the continuous use of such applications is limited due to the challenge of transmitting over highly-dynamic vehicular wireless channels. In such networks, the increasing availability of different frequency bands with correspondingly diverse propagation characteristics could allow flexibility and robustness of vehicular links. Even with spectral flexibility, links are extremely tenuous, demanding instantaneous decisions to remain connected, motivating an algorithm that can find the appropriate frequency band quickly and according to the current environmental context.

Clearly, more available spectrum could improve the performance for both links and networks. The FCC has approved the use of broadband services in the white spaces of UHF TV bands, which were formerly exclusively licensed to television broadcasters. These white space bands are now available for unlicensed public use, enabling

the deployment of wireless access networks across a broad range of scenarios from sparse rural areas (one of the key applications identified by the FCC) to dense urban areas [42]. The white space bands operate in available channels from 54-806 MHz, having a far greater propagation range than WiFi bands for similar transmission power [16]. In WiFi and white space heterogeneous wireless network, the service area degree of an access point depends on the capacity of radios, the propagation range and the demands of the serving area. The scant frequencies of radios, the propagation distinctive and the demands diversity of population distribution bring the variation of an access point service area. These issues are substantial to designing an optimal network deployment and provide potential commercial wireless services to clients in any location.

White space frequencies is not only benefit the access tier network, but also provides opportunity for backhual tier networks. About a decade ago, numerous cities solicited proposals from network carriers for exclusive rights to deploy city-wide WiFi, spanning hundreds of square miles. While the vast majority of the resulting awarded contracts used a wireless mesh topology, initial field tests revealed that the actual WiFi propagation could not achieve the proposed mesh node spacing. As a result, many network carriers opted to pay millions of dollars in penalties rather than face the exponentially-increasing deployment costs (e.g., Houston [72] and Philadelphia [22]). Thus, while a few mesh networks have been deployed in certain communities [20, 10], wireless mesh networks have largely been unsuccessful in achieving the scale of what was once anticipated [48]. Around the same time, the digital TV transition created more spectrum for use with data networks [5]. These white space bands operate in available channels from 54-806 MHz, having increased propagation characteristics as compared to WiFi [16]. Hence, the FCC has identified rural areas as a key application for white space networks since the reduced population from major metropolitan

areas allows a greater service area per backhaul device without saturating wireless capacity. Naturally, the question arises for these rural communities as well as more dense urban settings: how can the emerging white space bands improve large-scale mesh network deployments? While much work has been done on deploying multihop wireless networks with multiple channels and radios, the differences in propagation have not be exploited in their models [68, 83, 80], which could be the fundamental issue for the success of mesh networks going forward.

As white space frequencies are made available for wireless communication, both the academic and industry experts are seeking an integrated approach for white space and WiFi bands in wireless links and networks. In this work, we seek to jointly use white space bands and WiFi bands in vehicular and large scale network deployments. We also propose prospective graph theory solution for white space spectrum in short future.

1.1. Challenges

Wireless links and networks suffer from the limited available resources and interference. Everyone must share the bandwidth. Here, users and work carriers alike seek better service and lower cost for wireless networks. Spectrum agility offers a new promising resource to address these issues.

First, accurate knowledge of channel state is challenging to obtain due to the time varying nature of channel quality and interference. at the receiver. In recently, cognitive radio mechanisms which interleave channel accesses motivate the frequency band selection problem of finding the optimal spectrum on which to transmit [34]. Prior work has considered a number of challenges in leveraging white space frequencies including spectrum sensing, frequency-agile operation, geolocation, solving stringent spectral mask requirements, and providing reliable service in unlicensed and dynami-

cally changing spectrum [78]. In particular, there has recently been an acceleration in spectrum sensing work [70, 49, 19]. Based on these works, protocols have been built for multi-channel and/or multiband wireless operation [47, 71, 76]. Other works have presented methods for searching for the most efficient transmission channel [59], discovering channel information [70, 76], and estimating channel quality [47]. Moreover, the emergence of a number of diverse sensors on a vehicle motivates work on heterogeneous wireless networks, which have different frequency bands and technologies [41]. Thus, the various communication standards have diverse throughput capacity, allowing the choice of technology to possibly usurp frequency band decisions. For example, an 802.11n link at 5.8 GHz with high levels of loss might still be a better choice than a Bluetooth link at 2.4 GHz with little loss due to the discrepancy of hundreds of Mbps in throughput capacity. While these works have considered spectral activity and developing protocols and algorithms to find spectral holes, less of a focus has been on coupling such information with historical performance in a given propagation environment.

Second, in access layer network deployment, specific to rural areas, the lack of user density and corresponding traffic demand per unit area as compared to dense urban areas allows greater levels of spatial aggregation to reduce the total number of required access points, lowering network deployment costs. In densely populated urban areas, the greater concentration of users and higher levels of traffic demand can be served by maximizing the spatial reuse. While many works have worked to address multihop wireless network deployment in terms of maximizing served user demand and/or minimizing network costs, the unique propagation characteristics and the interference from coexisting activities in white space bands have either not been jointly studied or assumed to have certain characteristics without explicit measurement [80]. Specifically, previous work has investigated wireless network deployment in terms

of gateway placement, channel assignment, and routing [40, 55]. However, each of these works focus on the deployment in WiFi bands without considering the white space bands. Moreover, the assumption of idle channels held in these models fails to match the in-field spectrum utility, which could degrade the performance of a wireless network. These two issues are critical for designing an optimal network deployment and providing commercial wireless services to clients in any location.

The larger propagation range of white space channels is able to adapt channel association of users located in large area. When the users distributed in a large area, the temporal diversity and spectral diversity become key issues in white space wireless network applications. In sparse rural areas, plenty of white space channels are able to deploy new white space network. However, in dense area, the number of white space channels are restricted by FCC in a small number, such as there is none white space channel available in New York downtown [36]. The carrier have deploy WiFi wireless networks in the dense area. Other than the plenty white space channels and none white space channel extreme cases, most areas of major cities in the United States have one to eight white space channels [36]. These white space channels are able to complement the WiFi wireless networks to achieve better performance in coverage, power consumption, etc. Thus, exploiting these limited white space resource to improve the WiFi network in dense area is a perspective option for wireless networks. The white space frequencies offer not only more wireless capacity but also the convenience of access across large area for the heterogeneous wireless network structure. A single white space channel is able to satisfy all the users in the area when the total traffic demands of the users in the area are relatively low. The WiFi radios in the heterogeneous structure could be turned off for power saving. While when the total traffic demand of the users in the area is high, all the radios in the wireless network have to operate for the service of users. However, the amount of

traffic demands generally come across somewhere between these extremes. Thus, the question comes out, *in what degree the white space help to reduce the power consumptions of an existing WiFi mesh?* Especially when the WiFi mesh located in dense area with less white space channel availability.

Moreover, in the backhual layer, researchers have done both centralized and distributed work for channel assignment and routing [68, 87]. However, the FCC's new policy bring new opportunities and challenges for these issues. Increased channel capacity and propagation diversity forces new consideration for existing solutions. Since even the original multichannel problem has been proved to be NP-hard which could not be solved in polynomial time, low complexity solution for joint white space and WiFi usage is needed. As shown in Google database [7], the additional number of available white space frequency channels vary from city to city in US. Existing channel occupancy discussed in previous work [64] has shown that the occupancy of frequency impacts on wireless network deployment. Naturally, the question arises for improving the performance as well as the optimization of utilization: *how can the emerging white space bands improve large-scale mesh network deployments?* While much work has been done on deploying multihop wireless networks with multiple channels and radios, the differences in propagation have not been exploited in their models [83, 54, 27], which could be *the* fundamental issue for the success of mesh networks going forward.

Moreover, the joint use of WiFi and white spaces in access points depends on the capacity of radios, the propagation range and the demands of the service area. Thus, the new opportunities created by white spaces motivate the following questions for wireless Internet carriers, which have yet to be addressed: *(i) To what degree can white space bands reduce the network deployment cost of sparsely populated rural areas as opposed to comparable WiFi-only solutions?* and *(ii) To what degree can*

heterogeneous access points benefit the dense population areas and sparsely populated rural areas?

1.2. Contributions

This work proposes spectrum adaptation for both the wireless links and large scale network deployments to improve the performance of wireless devices in multiple frequency bands.

For link adaptation, we develop multiband protocols which couple the prior knowledge of in-situ performance of various bands with the instantaneous knowledge of spectral activity, SNR, and the current location of each band to arrive at a decision for the optimal band on which to transmit. To do so, we use an off-the-shelf platform that allows direct comparison and simultaneous experimentation across four different wireless frequency bands from 450 MHz to 5.8 GHz with the same physical and media access layers. We first develop a framework for multiband adaptation using both historical information and instantaneous measurements. This framework is broad enough to study adaptation across licensed and unlicensed bands, including white space frequency bands. We propose two different machine-learning-based multiband adaptation algorithms. The first machine learning algorithm, referred to as the Location-based Look-up Algorithm, is based on the idea of k-nearest-neighbor classification. The second machine-learning-based algorithm uses decision trees for classification. For comparison, we also create two baseline adaptation algorithms which attempt to make the optimal band selection based on only: (i.) historical performance data, and (ii.) instantaneous SNR measurements across various bands. We perform extensive outdoor V-2-V experiments to evaluate the proposed algorithms. Our results indicate that the proposed machine learning based algorithms improve throughput by up to 49.3% over these baseline methods.

In the access layer network deployment, we perform a measurement study which considers the propagation characteristics and observed in-field spectrum availability of white space and WiFi channels to find the total number of access points required to serve a given user demand. Across varying population densities in representative rural and metropolitan areas, we compare the cost savings (defined in terms of number of access points reduced) when white space bands are not used. To do so, we first define the metric to quantify the spectrum utility in a given measurement location. With the in-field measured spectrum utility data in metropolitan and surrounding areas of Dallas-Fort Worth (DFW), we calculate the activity level in WiFi and white space bands. Second, we propose a measurement-driven framework to find the number of access points required for areas with differing population densities according to our measurement locations and census data. We then evaluate our measurement-driven framework, showing the band selection across downtown, residential and university settings in urban and rural areas and analyze the impact of white space and WiFi channel combinations on a wireless deployment in these representative scenarios. The main contributions of our work in this part are as follows: We perform in-field measurements of spectrum utilization in various representative scenarios across the DFW metroplex, ranging from sparse rural to dense urban areas and consider the environmental setting (e.g., downtown, residential, or university campus). We develop a measurement-driven Multi-band Access Point Estimation (MAPE) framework to jointly leverage propagation and spectrum availability of white space and WiFi bands for wireless access networks across settings. We analyze our framework under capacity and coverage constraints to show that, with white space bands, the number of access points can be greatly reduced from WiFi-only deployments by up to 1650% in rural areas. We quantify the impact of white space and WiFi channel combinations to understand the trade offs involved in choosing the optimal channel setting, given

a certain number of available channels from multiple bands. Furthermore, we discuss to centralized using frequencies or distributed using them in single access point. Through our numerical simulation, we show that in dense area centralized using spectrum gain more than sparse area. For the heterogeneous access tier optimization, we perform a relaxed linear program which considers the variation of heterogeneous access point service area to find the lower bound total number of access points required to serve a given user demand. Further, we represent an Multiband Heterogeneous Access Point Deployment (MHAPD) greedy algorithm to approach the lower bound. Across varying white space and WiFi radios combination, population densities in representative rural and metropolitan areas we compare the cost savings (defined in terms of number of access points reduced) when white space bands are not used. We then evaluate our MHAPD algorithm, showing the heterogeneous band selection across downtown, residential and university settings in urban area and rural areas and analyze the impact of white space and WiFi combinations on a wireless deployment in these representative scenarios. The main contributions of our work in this topic include: We develop an optimization framework based on linear programming to jointly leverage white space and WiFi bands approaching the lower bound in terms of the number of access points to serve the demands of a given area. We design a MHAPD greedy algorithm, which models the problem as a bin packing problem. We evaluate the performance of the presented algorithm, comparing with the lower bound and the hexagon of WiFi access point deployment in sparse rural areas given similar channel resources. The numeric results shows that our algorithm gains 260% against the linear hexagon of deployments. We further analyze the performance of heterogeneous access point performance across variety of population densities. The numeric results show that heterogeneous access points which jointly use white space and WiFi bands could improve the budget saving up to 323%.

In the scant white space resouce scenarios, we study the white space resource impacts on mesh network power consumption via queuing theory model. We describe the heterogeneous wireless network structure with both white space bands and WiFi bands. We formulate the system as a queuing model. We analyze the heterogeneous structure under the the waiting time constraint for resource allocation in multiple scenarios of the structure. We further propose a Greedy Server-side Replace (GSR) algorithm to minimize the power consumption for the heterogeneous network structure. We then evaluate the algorithm, showing the power consumption gains across sparse and dense areas and analyze the impact of the number of white space and WiFi channels in these representative scenarios. We perform 24 hours in-field measurements in neighborhoods, campus, downtown business building, and urban business buildings. Through these in-field measurements, we estimate the achieved channel capacity of these typical area in north Texas. We leverage the user mobility footprint through in-filed Android based WiEye measurements of Dallas area on weekdays. Through the measurements analysis, we tell the user distribution in multiple types of areas across 24 hours in weekdays. We formulate the heterogeneous wireless structure as a queuing system. Based on previous queuing theory works, we analyze the resource allocation of the system quality of service in waiting time. Based on the analysis, we propose a Greedy Server-side Replace (GSR) algorithm to allocate the channel resource to minimize the power consumption. We perform measurement-driven numerical simulations to analyze various scenarios of channel resource and users distribution. Our results shows that the white space bands reduce the power consumption in sparse area by up to 512.55% in weekdays.

In the backhual layer network deployment, we leverage the diversity in propagation of white space and WiFi bands in the planning and deployment of large-scale wireless mesh networks. To do so, we first form an integer linear program to jointly

exploit white space and WiFi bands for optimal WhiteMesh topologies. Second, since similar problem formulations have been proved to be NP-hard [45], we design a measurement driven heuristic algorithm, Band-based Path Selection (BPS). We then apply the approaching method in multiple scenarios with in-field measurement data. Across a wide range of scenarios, including network size, population distribution, deployment distance gap, we exploit when and how to emerge white space bands in mesh networks. The performance of our scheme is compared against two well-known multi-channel, multi-radio channel assignment algorithms across these scenarios, including those typical for rural areas as well as urban settings. We further discuss how the channel occupancy impacts on wireless networks and show the comparison of our algorithm and previous methods in typical scenarios. Finally, we quantify the degree to which the joint use of both band types can improve the performance of wireless mesh networks. We analyze the white space bands application in wireless network deployment and develop an optimization framework based on integer linear programming to jointly leverage white space and WiFi bands to advantages and disadvantages in wireless mesh networks with measured channel occupancy. We build a heuristic measurement driven algorithm, Band-based Path Selection (BPS), which considers the diverse propagation, overall interference level of WiFi and white space bands with measurement adjust. We perform extensive analysis across offered loads, network sizes, mesh nodes spacing and WiFi/white space band combinations, to compare against previous multichannel multiradio algorithms. We discuss the channel occupancy and mesh spacing impacts the performance of similar channel resources (bandwidth and transmission power), We show the improvement of our BPS algorithm in typical configurations up to 180% versus. previous multichannel algorithms.

In the future, we propose to find a better solution based on graph theory for multiband wireless network deployments. Future work will provide a mechanism for not only channel assignment, but also where we should locate the gateway nodes with a less complex solution to achieve a complete framework for multiband wireless network deployment.

1.3. Thesis Overview

In Chapter 2, we discuss the background of this work, including the basic knowledge related to this work and the hardware platform and software tools applied in our research. Chapter 3 provides an analysis and solution of vehicular link adaptation across multiple frequency bands. We also propose an access network deployment framework in Chapter 4 and discuss the optimization of a single access point with spectrum limitations. Then, we further compare this solution to one which both white space bands and WiFi bands to quantify the benefit of white spaces. In Chapter 6, we propose an algorithm to assign channels in multiband wireless network scenarios for optimizing the throughput performance in multihop backhual networks. Further, we quantify the heterogeneous application of white space bands and WiFi bands in access points deployment process. In Chapter **??**, we propose the future in multiband network deployment using graph theory for locating gateway nodes. Finally, we conclude our work in Chapter 8.

Chapter 2

Background

In this chapter, we describe the background of our research, including the basic technology related to this work, the hardware and software tools that we used to implement and evaluate our proposed algorithms in this work.

2.1. White Space Bands

The white space band term is mentioned the frequencies channels previously used by analog TV broadcasts. In United States, full power analog television broadcasts, which operated between the 54 MHz and 806 MHz television frequencies (Channels 2-69), ceased operating on June 12, 2009 per a United States digital switchover mandate. At that time, full power TV stations were required to switch to digital transmission and operate only between 54 MHz and 698 MHz. [5]

Industry and academia have recognized the value of white space bands in wireless communication. Various proposals, including IEEE 802.11af, IEEE 802.22 and those from the White Spaces Coalition, have advocated using white spaces left by the termination of analog TV to provide wireless broadband Internet access. Some company from industry has designed device intended to use these new available channels as a "white-spaces device" (WSD), such as Ubiquiti SR serials products. These devices are designed to detect the presence of existing but unused areas of airwaves, such as those reserved for analog television, and utilize these unused airwaves to transmit signals for data traffic. Such technology is predicted to improve the availability of broadband Internet service, especially in rural areas.

White space bands and ISM WiFi bands have great variation of propagation characteristics. Wireless propagation refers to the signal loss characteristics when wireless signals are transmitted through the wireless medium. The strength of the received signal depends on both the line-of-sight path (or lack thereof) and multiple other paths that result from reflection, diffraction, and scattering from obstacles [13]. The widely-used Friis equation characterizes the received signal power P_r in terms of transmit power P_t, transmitter gain G_t, receiver gain G_r, wavelength λ of the carrier frequency, distance R from transmitter to receiver, and path loss exponent n according to [32]:

$$P_r = P_t + G_t + G_r + 10n \log_{10} \left(\frac{\lambda}{4\pi R} \right) \tag{2.1}$$

Here, n varies according to the aforementioned environmental factors with a value ranging from two to five in typical outdoor settings [69].

According to Eq. 2.1 white space band not only provide more bandwidth for wireless communication, but also bring the diversity in transmission/interference range. Our algorithms and frameworks try to exploit white space bands advantages of link communication and network deployment through spectrum agility with WiFi bands.

2.2. Spectrum Utilization

When access a channel licensed by FCC, most of the time we could detect signals in the air from devices who share the channel. To represent the utilization level of a channel, we define *activity level*, A, as the percentage of time when the channel is occupied by all competing sources $x_j (j = 1, 2, 3, ...)$ other than the intended transmitter y. For 802.11-based transmissions, the activity level on band i is defined as:

$$A^i = \frac{\sum_j \sum_k \frac{L_k^{x_j}}{R_k^{x_j}}}{\sum_k \frac{L_k^y}{R_k^y} + \sum_j \sum_k \frac{L_k^{x_j}}{R_k^{x_j}} + S\sigma} \tag{2.2}$$

where $L_k^{x_j}$ and $R_k^{x_j}$ represent the packet length in bits and data rate at which that packet is transmitted, for external sources x_j; S and σ are the number of idle slots and slot duration, respectively. When considering the activity level of non-802.11 users (*e.g.*, the bands currently licensed to TV), we use the received signal level from non-802.11 interfering sources P_N^i on band i directly as an input to our algorithms.

In practical, we get the activity level through in-field measurements. The measurements process will be introduced in following chapters. We define the percentage of sensing samples (S_θ) above an interference threshold (θ) over the total samples (S) in a time unit as the activity level (A) of inter-network interference:

$$A = \frac{S_\theta}{S_a} \tag{2.3}$$

The capacity of a clean channel is denoted by C. With the protocol model, the capacity of a channel with inter-network interference C_r could be represented as the remaining free time of the channel capacity according to:

$$C_r = C * (1 - \bar{A}) \tag{2.4}$$

2.3. WiEye Measurement Platform

WiEye application created for the data collection is currently available for download and usage via the Google Android Market under the name WiEye. The application offers WiFi access points connection quality in both graphical and tabular form. All data collection is done in the background, either continuously while the user is running the application or periodically if the user has opted in to background data collection to SMU research. The data collected has been approved by the Southern Methodist University Institutional Review Board, a human subjects research committee,ensuring that all ethical precautions have been taken in collecting data from the users of our application.

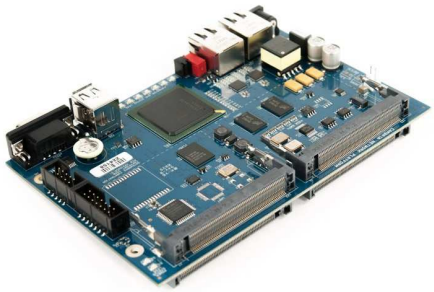

Figure 2.1: The Gateworks GW2358 off-shelf Platform.

2.4. Gateworks Platform

The off the shelf platform we use for our measurements is the GW2358. GW2358 is a member of the Gateworks Cambria Single Board Computer family. The GW2358 meets the requirements for enterprise and residential network applications. This single board computer consists of an Intel IXP435 XScale operating at 667MHz, 128Mbytes of DDRII-400 DRAM, and 32Mbytes of Flash. Peripherals include four Type III Mini-PCI sockets, two 10/100 Base-TX Ethernet ports with IEC-6100-4 ESD and EFT protection, two USB Host ports, and Compact Flash socket. Additional features include digital I/O, serial EEPROM, real time clock with battery backup, system monitor to track operating temperature and input voltage, RS232 serial port for management and debug, and watchdog timer. The GW2358 also supports GPS and RS485 serial port as ordering options. Power is applied through a dedicated connector or through either Ethernet connector with the unused signal pairs in a passive power over Ethernet architecture. An open source software OpenWrt board support package is included for Linux operating systems.

The Gateworks platform works with Ubnt radios to perform 802.11 multiband measurements for both indoor and in-field. It helps to collect the SNR, throughput

Figure 2.2: Rohde & Schwarz FSH 8 Spectrum Analyzer.

and packet information for the post process.

2.5. Rohde & Schwarz FSH8 Spectrum Analyzer

The R&S FSH 8 spectrum analyzer is designed portable for application in multiple environment, especially for in-field measurement. Its low weight, its simple, well-conceived operation concept and the large number of measurement functions make it an indispensable tool for anyone who needs an efficient measuring instrument for outdoor work. We employ FSH 8 in our indoor and outdoor measurements to collect data in multiple bands.

FSH 8 is able to sense the signal in the air from 9 KHz to 8 GHz. The spectrum analyzer could sense both 802.11 signals and non-802.11 signal in the air. Through the time stamp, we could merge data from Gateworks platform and FSH8 platform to perform our algorithms and frameworks.

2.6. Mesh Network Deployment

A wireless mesh network is a common infrastructure for providing wireless access for clients by the network carriers. Wireless mesh networks is made up of multiple radios which organize in a mesh topology. Each node forwards messages on behalf of the other nodes. The nodes connected to clients are referred to as the access tier. The

nodes to relay data traffic to wired networks are referred to as the backhual tier. For the access tier, the nodes need to cover the service area and provide sufficient capacity for the clients in target area. The backhual tier needs to have a highly-efficient path to the wired network which can potentially shorten multiple wireless hops. We analyze mesh network deployments in a scenario which includes multiple frequency bands, and propose our solutions for access and backhual network deployment.

Chapter 3

Vehicular Link Spectrum Adaptation

In this section, we first formulate the multiband adaptation problem in vehicular wireless links and introduce the set of information we use to make band decisions, which we refer to as context information. We then propose two machine-learning-based multiband adaptation algorithms for vehicular channels. For comparison, we also propose two baseline adaptation methods based on existing solutions which consider historical and instantaneous information independently.

3.1. Link Adaptation Problem Formulation

Consider a system with n frequency bands, represented by an index set $\{1, 2, \ldots, n\}$. The objective is to select the optimal band, b_{best}, to transmit at each time instant that maximizes a desired objective function such as throughput. The throughput r_i on band i depends on several factors such as received signal power P_R^i, noise power P_N^i, the channel activity level A^i, the velocity of the transmitter, v_{tx}, the velocity of the receiver, v_{rx}, and location information which depends on each algorithm and will be specified in the algorithm section. The aforementioned set of all information used to make multiband decisions composes the users context. This relationship is represented in general as $r_i = f(P_R^i, P_N^i, A^i, v_{tx}, v_{rx}$,context information per algorithm). The objective can be stated as:

$$b_{best} = \arg\max_i r_i \tag{3.1}$$

The framework differentiates interference from other nodes using the same technology (via the Activity level A^i) and other technologies (via the noise level P_N^i). For

instance, an 802.11 node can decode the packets of other 802.11 nodes but can only sense instantaneous noise levels from ZigBee/Bluetooth nodes. Decoding the packets can provide increased knowledge such as data rate and packet size to determine the duration of the channel use. We can exploit the long-term behavior by using historical performance data for the collected context information (*e.g.*, v_{tx}, v_{rx}, A^i, P_N^i, P_R^i) [58].

3.2. Multiband Adaptation Algorithms

In order to evaluate the proposed multiband adaptation algorithms, we construct two baseline methods: (i.) We search for the most commonly selected band as the best band in the historical data and choose it as the final band decision. (ii.) For each band, we build a lookup table for throughput T_{ideal} in an idealized channel given the $RSSI$ and obtain the best band according to following:

$$\max_i \ T_{ideal}^i \times (1 - A^i), \tag{3.2}$$

The throughput T_{ideal} is measured with an Azimuth ACE-MX channel emulator [3]. The details of the system setup and data collection are discussed in Section 3.3.

Machine learning has been used as an important tool in wireless communications [39]. When a user enters an area, the machine learning algorithm can learn from the historical data and select the potential optimal band given the input, *e.g.*, P_R^i, v and P_N^i. We propose two multiband adaptation algorithms based on two machine learning methods: k-nearest neighbor (KNN) and decision trees.

Location-based Look-up Algorithm. KNN is a machine learning method based on searching for the closest training data points in the feature space and various modified versions have been applied successfully for classification [91]. In the *Location-based Look-up Algorithm*, we search for the closest neighbors of a testing point by using each parameter one by one in the input set. The *Location-based Look-up Algorithm*

additionally involves geographic information for band selection other than received signal power P_R^i, noise power P_N^i, the activity/occupancy level A^i, the velocity of the transmitter, v_{tx}. The performance of the selected training data points is averaged to generate an estimate of the performance at each band. Then the band with the highest throughput performance is selected as b_{best}.

For the *Location-based Look-up Algorithm*, context information involves the location g (GPS latitude and longitude), v, P_R^i, P_N^i and A^i. To make a band prediction, we have four look-up blocks to reduce the training data points which are similar to the testing data point. First, we search for the historical data which is closest to the testing data based on GPS location. If the number of found historical data points is less than a predefined threshold, θ_{AArea}, we increase the distance range (the actual threshold is discussed in Section 3.3). Then, based on the filtered historical data, we collect θ_{AArea} data points which are closest to P_R^i, where θ_{AArea} is the threshold of the number of collected data points. A similar process is repeated based on P_N^i and v, respectively. After deciding the final data set, we average the throughput of data points at each band. This algorithm's key steps are shown in Algorithm 3.1.

Region-based Decision Tree Algorithm. Decision trees are a widely-used machine learning algorithm due to their low complexity and stable performance [17]. A decision tree can model the relationship in the training data between the context information and the optimal band as a set of tree-like deduction structures. Before implementing the training process, we prepare a training set including a group of training data points of $\{v_{tx}, v_{rx}, P_R^1, ..., P_R^n, A^1, ..., A^n, P_N^1, ..., P_N^n, b_{best}\}$ based on the collected measurements. We obtain b_{best} by comparing the throughput performance of all available bands and selecting the band with the highest throughput. We choose the C4.5 algorithm to generate our decision tree [38], a widely-used algorithm based on the information entropy gain.

Algorithm 3.1 Location-based Look-up Algorithm

Input:

g: Location information of multiband node

θ_{Area}: Threshold of a location

θ_{RSSI}: Threshold of RSSI

$\theta_{Velocity}$: Threshold of velocity

$\theta_{set} = \{\theta_{AArea}, \theta_{ARSSI}, \theta_{ANon802.11SI}, \theta_{AVelocity}\}$: Threshold of data amount for {a location, RSSI, non-802.11 interference, velocity}

$D^i \in \{D^1, D^2, \ldots, D^n\}$: Historical look-up data

1: **for** $i <= n$ **do**

2: Initialize $Data_{Location}, Data_{RSSI}, Data_{Velocity}$ to zero matrix;

3: **for** $j <= m$ **do**

4: $Amount = Amount^j_{\{Data_{Location,i}, Data_{RSSI,i}, Data_{P_N,i}, Data_{Velocity,i}\}}$;

5: $\theta = \theta^j_{set}$;

6: **while** $Amount < \theta$ **do**

7: $Data_{Location,i} \leftarrow f_{Lookup}(D^i, g, \theta_{Area})$: Find data in D^i whose distance less than θ_{Area};

8: $\theta_{Area} = \theta_{Area} \times 1.1$;

9: **end while**

10: $T_{a,i} = avr(Data_{Velocity,i})$;

11: $T_{e,i} = T^i_a \times (1 - A^i)$;

12: **end for**

13: **end for**

14: $b_{best} = \max_i\{T^1_e, \ldots, T^i_e, \ldots, T^n_e\}$;

Output:

b_{best}: Optimal transmission band

At each intermediate node in the decision tree, the learning algorithm calculates the information entropy gain of splitting the remaining training data points based on each parameter in the input set, *e.g.*, P_R^i, v or P_N^i. Then, it compares and selects the parameter with the highest entropy gain to decide the test condition at each intermediate node until all training data points are classified. The leaf nodes indicate the optimal band for prediction in our application. Then, the trained decision structure is integrated into the transmitter protocol stack. With the collected context information, the decision structure can suggest the band with the best throughput performance.

The relationship between the context information and the best band could differ at different locations because of diverse propagation environment characteristics. To reduce the heterogeneity of training data from different locations, we split the vehicular route into several regions and implement the training process based on the historical data collected in each region. Then, the trained decision structure is integrated in our system for multiband adaptation in each region. The granularity of regional division is one parameter that affects the training set as well as the performance of the resulting decision tree. We evaluate the granularity of these divisions in Section 3.3.

3.3. Experiments for Multiband Algorithms

To study these algorithms, we have developed indoor and in-field experiments on a Linux-based 802.11 testbed [4]. The platform includes a Gateworks 2358 motherboard with Ubiquiti XR radios (XR9 at 900 MHz, XR2 at 2.4 GHz, XR5 at 5.2 GHz) and a DoodleLabs DL475 radio at 450 MHz [2, 6]. We use an Azimuth ACE-MX channel emulator for controllable propagation and fading characteristics with a broad range of industry-standard channel models from 450 MHz to 5.9 GHz [3].

3.3.1. In-lab Experiments for Radio Characterization

To establish an SNR-to-throughput relationship for the *SNR-based Throughput Look-up Algorithm*, we use an experimental setup where two wireless nodes communicate across repeatable emulated channels generated by the channel emulator (Figure 3.1). For a given band and card, we measure the throughput of a fully-backlogged UDP flow using the *iperf* traffic generator. We use constant attenuation over an idealized channel condition and repeat the experiment to produce various RSSI values. Despite the same physical and media access control layers of the radios, there are slight differences in the throughput achieved per radio at the same attenuation level. Thus, we normalize these throughput values to have the same maximum throughput across radio types.

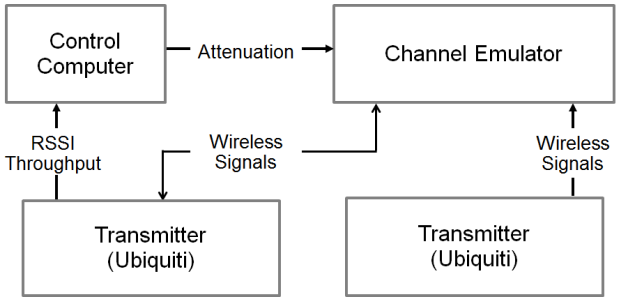

Figure 3.1: Experimental setup for channel emulator.

3.3.2. Experimental Design for In-field Data Collection

We now describe the in-field experimental design to obtain a data set for evaluating our multiband algorithms. Two Gateworks boards, each containing the aforementioned four radios, are installed on two cars. One node is always the receiver and at a fixed location. The other node is always the transmitter and travels around the block of a public park as shown in Figure 3.2. One loop of the route will be used as a unit of training in the next section.

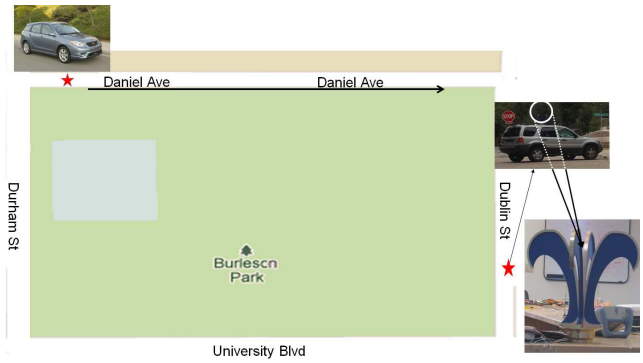

Figure 3.2: In-field Experimental Setup.

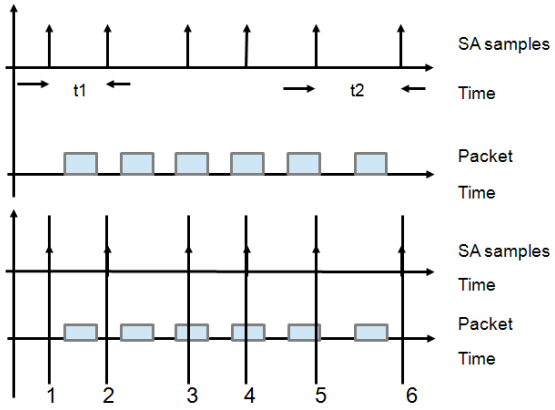

Figure 3.3: Spectrum Analyzer Data Processing.

During each loop, the transmitter sends a fully-backlogged UDP flow using *iperf* on each of the four radios simultaneously. To focus on band selection and ensure the greatest range, we disable autorate and use a fixed data rate of 6 Mbps. The receiver continually performs a *tcpdump* of all received 802.11 packets [44]. Additionally, a QH 400 Quad Ridge Horn Antenna (shown in Figure 3.2) is connected to a Rhode & Schwarz FSH8 mobile spectrum analyzer at the receiver to monitor spectral activity. Then, based on the time stamps, we remove 802.11 packets from the spectral trace so that only non-802.11 interference will contribute to P_N^i.

Figure 3.3 shows how we obtain the non-802.11 interference, P_N^i. We expunge the spectrum analyzer (SA) samples which overlap in time with the dumped 802.11 packets, such as packets 3, 4, and 5. Then, the reported interference value will not contain the received power from 802.11 packets, which have already been considered via the activity level, A.

The in-field data is processed offline where data from all instruments involved is synchronized based on the GPS time stamps. As discussed in Section 3.3.1, the throughput of each radio is normalized based upon emulator experiments to account for any manufacturing differences.

3.4. Performance Analysis of Algorithms

We now evaluate our proposed algorithms with the experimental setup described in Sections 3.3.1 and 3.3.2. The metrics of *Accuracy* and *Throughput Gap* are used in the evaluation. We consider each second of the in-field trace and observe the frequency band that had the highest throughput. The *Accuracy* is defined as the percentage of best band predictions that match the observed optimal band, where a prediction is made each second. Conversely, the *Throughput Gap* is defined as the difference between the throughput observed on the optimal band and the throughput achieved by the predicted best band over the throughput of the observed optimal band. In the situation where the optimal band is not chosen, the throughput could be close between the chosen and optimal bands, meaning that the incorrect band choice did not result in a large throughput loss. Thus, the *Throughput Gap* metric captures the severity of the incorrect choice.

Since the *SNR-based Throughput Look-up Algorithm* requires only emulator-based training, the *Accuracy* and *Throughput Gap* can be calculated for all loops of the in-field trace. However, the *Location-based Look-up Algorithm* and *Region-based Decision*

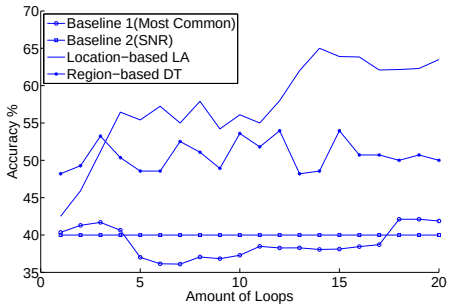

Figure 3.4: Accuracy of the four multiband algorithms.

Tree Algorithm require in-field training. Thus, the data set must be divided into a training set and testing set for evaluation.

In Figure 3.4, we show the aforementioned *Accuracy* of the four multiband algorithms in selecting the band with the highest throughput. The x-axis represents the number of loops around the block of the mobile transmitter (shown in Figure 3.2) that will be used by the machine-learning-based algorithms. We use the same training and testing set to compare the *Location-based Look-up Algorithm* and *Region-based Decision Tree Algorithm*. From the results, we observe the following:

- At each loop, the first baseline algorithm, *Most Commonly-Selected Band*, uses the band with the greatest long-term average of the percentage of time that band yields the highest throughput over the previous loops. The accuracy ranges from 36.1% to 42.9%.

- The second baseline algorithm, *SNR-based Throughput Look-up*, maintains 39.2% across all the loops since it relies only on emulator-based training.

- The *Region-based Decision Tree Algorithm* has an accuracy ranging from 48.2% to 54.0% but contains many dips due to the relationship between the context information and the distribution of the best band choice changing on a loop-by-loop basis. Additional training data slightly improves the decision structure overall but primarily induces additional noise in the training process.

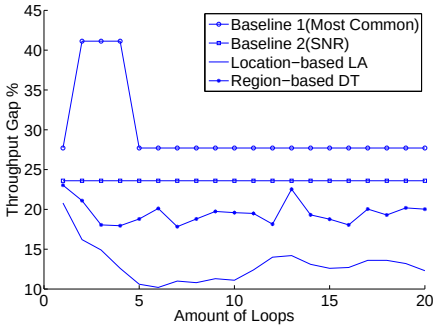

Figure 3.5: Throughput Gap of the four multiband algorithms.

- The *Location-based Look-up Algorithm* begins with an accuracy of 42.5% but improves the most out of any algorithm to finish with an accuracy 62.5% with the highest accuracy of 65.0% occurring after loop 14. Additional in-field training loops are likely to further improve the multiband selection accuracy.

Figure 3.5, depicts the *Throughput Gap* of the four algorithms we evaluated and shows the following.

- The *Most Commonly-Selected Band Algorithm* has two different modes of throughput gap based upon which band has the highest long-term percentage. For loops 2-4, the choice is 5.8 GHz, which has a gap of 41.1% using the test set. For all other loops, the choice is 2.4 GHz, which has a gap of 27.7%.

- The *SNR-based Throughput Look-up Algorithm* shows a baseline performance of 23.6% for the throughput gap.

- The *Region-based Decision Tree Algorithm* benefits from additional training, going from a throughput gap of 23.0% to 20.0%. Spatial and temporal changes to context information bring dips to the curve as discussed earlier.

- Finally, the *Location-based Look-up Algorithm* takes only 6 loops of training to reach its lowest value of 10.2% in terms of throughput gap. From loops 1 to 20,

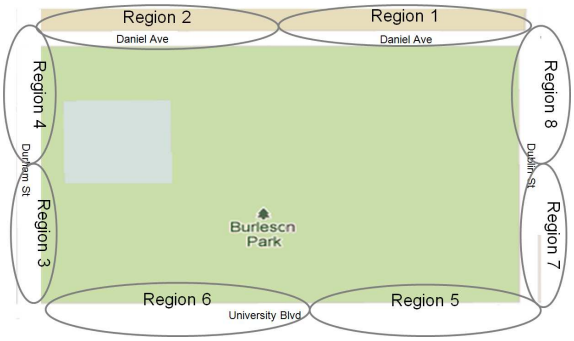

Figure 3.6: Spatially splitting experimental area into 8 regions.

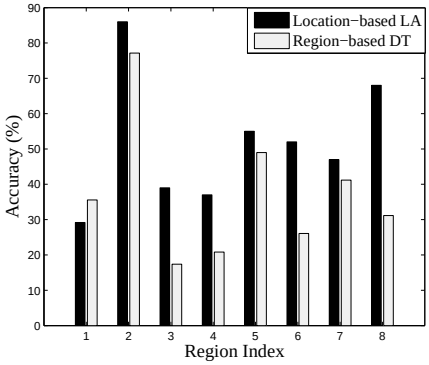

Figure 3.7: Accuracy when dividing training set into 8 regions.

the throughput gap goes from 20.8% to 12.3%, which might still be improved upon with additional training.

We now consider the effect of further sub-dividing in-field experimental testing data into regions for our *Location-based Look-up Algorithm* and *Region-Based Decision Tree Algorithm*. To do so, we divide the loop around the park into eight regions as shown in Figure 3.6, which has two competing effects: (i.) Smaller regions allow similar experimental data to be used in the training process, potentially improving the decision structure. (ii.) For a given training set, dividing it into regions reduces the number of training points for the machine learning algorithms, potentially weakening the decision structure. In Figure 3.7, we observe the *Accuracy* of the eight regions

for both algorithms.

- In all but Region 1, the *Location-based Look-up Algorithm* has better performance than *Region-based Decision Tree Algorithm*. The improved accuracy of the former algorithm can be attributed to its ability to distinguish each point's relative distance to the middle of the region For the *Region-based Decision Tree Algorithm* to capture such a notion, the regions would have to be further subdivided, increasing the number of trees and reducing the training set per tree.

- For this training set, the reduction in training data caused by the regional divisions had a net loss on the performance of the *Region-based Decision Tree Algorithm*. However, if the training set was much larger for a given area, the net effect of regional divisions could be positive.

3.5. Summary

In this chapter, we investigated multiband adaptation to leverage the propagation and context for vehicular applications. We did so by proposing two machine-learning-based schemes and compared their performance against two baseline schemes. In our experimental analysis, we evaluated the performance of these algorithms in the field on an off-the-shelf platform. Experimental results demonstrate that the proposed algorithms can achieve up to 49.3% greater throughput than the baseline algorithms with an accuracy up to 65%. In future work, we will study the impact that multiple diverse environments have on the training as well as evaluate the optimal use of multiple, diverse radios in unison.

Chapter 4

Spectrum Adaptation for Single Hop Access Networks

In this chapter, we illustrate the challenges of band selection in wireless network deployments and formulate the problem of band selection in wireless network deployments jointly using WiFi and white space bands. Further, we present a measurement-driven framework for estimating the access point number to serve the traffic demand of a given population.

4.1. White Space Opportunity and Challenge In Network Deployment

As described in Chapter 2, white space bands and WiFi bands have variation of propagation range making a great gap of communication range and interference range. Despite sufficient levels of received signal, interference can cause channels to be unusable (e.g., due to high levels of packet loss) or unavailable (e.g., due to primary users in cognitive radios [39]). Prior work has worked to reduce interference levels via gateway deployment, channel assignment, and routing [40, 83]. The interference of a wireless network could be divided into two categories according to the interfering source: *(i)* intra-network interference, caused by nodes in the same network, and *(ii)* inter-network interference, caused by nodes or devices outside of the network. Most of the existing works try to reduce the intra-network interference without regard to the inter-network interference [80]. However, the existence of inter-network interference becomes an important problem when considering the availability of white space bands. While theoretical models which describe inter-network interference exist, accurately characterizing a particular region must be done empirically.

When wireless devices operate in WiFi bands, the channel separation is relatively small (e.g., 5 MHz for the 2.4 GHz band). As a result, many works assume that the propagation characteristics across channels are similar. However, with the large frequency differences between WiFi and white space bands (e.g., multiple GHz), propagation becomes a key factor in the deployment of wireless networks with both bands. Here, a frequency band is defined as a group of channels which have little frequency separation, meaning they have similar propagation characteristics. In this work, we consider the diverse propagation and activity characteristics for four total frequency bands: 450 MHz, 800 MHz, 2.4 GHz, and 5.2 GHz. We refer to the two former frequency bands as white space bands and the two latter frequency bands as WiFi bands. The differences in propagation and spectrum utilization create opportunities for the joint use of white space and WiFi bands in wireless access networks according to the environmental characteristics (e.g., urban or rural and downtown or residential) of the deployment location.

Typically, the deployment of wireless access networks is subject to coverage and capacity constraints for a given region. Coverage is defined with respect to the ability of clients to connect to access points within their service area. We use a coverage constraint ratio of 95% in this work for a target area [73]. Capacity is defined with respect to the ability of a network to serve the traffic demand of clients. Spatial reuse allows improved capacity but increases the cost of deploying a network by increasing the total number of access points required. Hence, for densely-populated areas, the greatest level of spatial reuse possible is often desired. In contrast, sparsely-populated rural areas have lower traffic demand per unit area. Thus, aggregating this demand with the use of lower frequencies via white space bands could be highly effective in reducing the total number of access points required to achieve similar coverage and capacity constraints. Moreover, since less TV channels tend to be occupied in

sparsely-populated areas [8], a larger number of white space bands can be leveraged in these areas.

4.2. Model and Problem Formulation

As opposed to previous works such as [83, 90, 80], this paper focuses on reducing the inter-network interference for various population densities for wireless access networks which jointly employ WiFi and white space bands. We propose a measurement-driven framework to estimate the number of access points required for serving the traffic demand of a certain area. We assume an access point has a limited number of radios which operate on any channel of a fixed number of channels with the same antenna gain. Each radio on an access point operates with a classic protocol model [37]. We further assume that there is a given take rate and traffic demand for a given population (as specified in Section 4.3).

For spectrum utility and resulting channel availability, we use a long-term measurement for each band refeqn:80211activity. The capacity of a clean channel is denoted by C. With the protocol model, the capacity of a channel with inter-network interference C_r could be represented as the remaining free time of the channel as shown in Eq. 5.7.

A network deployment should ideally provide network capacity equal to the demand of the service area to maintain the capacity constraint. The demand of a service area could be calculated as the summation of individual demands all over the service area $D_a = \sum_{p \in P} D_p$. Since household demand for the Internet has been previously characterized [75], D_a could represent the population distribution f and service area k as $D_a = \sum_{f \in F, k \in K} \bar{D_p} * f * k$. The capacity constraint could be represented with an access point set M according to:

$$\sum_{m \in M} C_r^m \geq \sum_{f \in F, k \in K} \bar{D_p} * f * k \tag{4.1}$$

At the same time, the wireless network must additionally satisfy the coverage constraint in the service area where the access points provide connectivity for client devices. Generally, a coverage of 95% is acceptable for wireless access networks [73].

In a joint white space and WiFi scenario, the activity level varies according to various interfering sources and the propagation characteristics induced by the environmental characteristics of the service area. A simple method with the least number of access points to cover an area is to use multiple orthogonal lower-frequency channels. However, the FCC limits white space band availability for data networks in most metropolitan areas in the United States [7]. Moreover, the number of channels in each band is limited. Too many lower-frequency channels will cause high levels of intra-network interference for the network, which is out of our scope in this work. We assume that the cost of the network is proportional to the number of access points required for a given user demand (i.e., due to the cost of hardware and installation). Therefore, given a geographical region for a new network deployment, we build a measurement-driven framework called Multiband Access Point Estimation (MAPE) to compute the required number of access points.

In the space domain, the advantage of higher-frequency channels is the spatial reuse, while the lower-frequency channels provide greater levels of coverage. Generally, higher frequencies are more appropriate for populated areas, and lower frequencies are more appropriate for sparse areas. The temporal variation of spectrum utilization differs across bands. For an Internet service provider, the service quality which maps to the capacity constraint must be satisfied. Given a metropolitan area, the population distribution can be found according to census data [9]. Then, we can estimate the capacity demand of each type of area with the assumption that users will exhibit average demand. According to the population distribution, we split the area into different types, which compose the spatial input. Then, we use the measured

Algorithm 4.1 Multiband Access Point Estimation (MAPE)

Input:

A: Measured Activity Level

F: Population Distribution

C: Clean Channel Capacity

n: Path Loss Exponent

B: Available Frequency Bands

M: Area to be Covered

1: Split M in to different type, calculate the traffic demand density f

2: Calculate in-field channel capacity C_r as $C(1 - A)$

3: Get the propagation coverage area radius R_p from the Friis model based on n, B, F

4: Calculate the QoS coverage radius R_{QoS} of a multiband access point that satisfies the demands of the area

5: The coverage radius of a multiband access point is $MinR_p, R_{QoS}$

6: Apply a regular-hexagonal deployment to get the number of access points for serving given area M

Output:

The number of access points

activity level as the temporal input. We have an average channel capacity of each band according to the activity level. With the received signal strength threshold, the Quality-of-Service-constrained coverage area of different types per channel, and the spatial reuse distance can be directly computed. Then, the maximum area an access point could cover can be calculated as the minimal area of the QoS-based coverage area and propagation coverage. Then, the transmission power is adjusted to fulfill the coverage restriction subject to the FCC regulations for maximum-allowable transmit power. A classic regular-hexagonal deployment process is employed to place the access points.

4.3. Experiment and Analysis

To evaluate the spectrum utility from in-field measurements, we perform experiments with an off-the-shelf wireless platform and mobile spectrum analyzer. According to the measured data, we apply our MAPE framework to analyze the role of white space and WiFi bands in the total access points required for a given deployment area and user demand.

4.3.1. Experiment Design

We employ a Linux-based 802.11 testbed, which includes a Gateworks 2358 board with Ubiquiti XR radios (XR9 at 900 MHz, XR2 at 2.4 GHz, XR5 at 5.2 GHz) and a DoodleLabs DL475 radio at 450 MHz. We develop shell scripts which utilize tcpdump to enable the testbed to work as a sniffer, recording all 802.11 packets. However, since the Gateworks platform only updates its estimate of received signal strength upon the reception of a new packet (and not all relevant channel activity is 802.11 based), we employ a spectrum analyzer to form a notion of inter-network interference with finer granularity. Hence, we also use a Rohde & Schwarz FSH8 portable spectrum works from 100 KHz to 8 GHz. The portable spectrum analyzer is controlled by a Python script on a laptop to measure the received signal strength.

To the best of our knowledge, there is no readily available mobile, multiband antenna from 450 MHz to 5.2 GHz on the market. Thus, we use a 700-MHz mobile antenna to perform in-field measurements. We then normalize the mobile antenna performance across bands with indoor experimentation. To do so, we use a Universal Software Radio Peripheral (USRP) N210 to generate signals at 450 MHz, 800 MHz, and 2.4 GHz. We feed the USRP signals directly to a spectrum analyzer and adjust the configuration of USRP to make the received signal strength the same as the 5.2 GHz signal from Gateworks 2358 with a XR5 radio. Then, we connect the signal

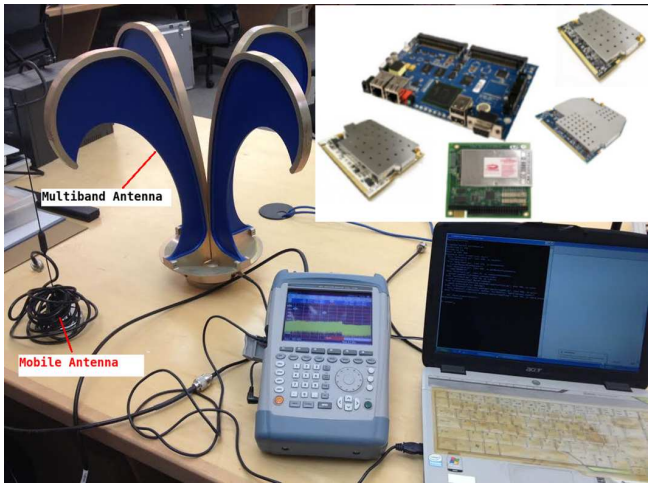

Figure 4.1: Multiband Measurement Platform

source to a fixed multiband antenna (QT 400 Quad Ridge Horn Antenna) and measure the received signal at a fixed distance with the 700 MHz antenna and antennas for different bands to obtain the antenna loss for each band. We adjust the received signal strength collected via the 700-MHz mobile antenna according to the normalization.

Our experimental platform is shown in Figure 4.1. The mobile spectrum analyzer records 32 samples per second on each band under test with appropriate time stamps. The Gateworks sniffer platform also records all the received WiFi packets according to their time stamps. The duplicate samples in WiFi bands from spectrum analyzer and Gateworks are deleted according overlapping time stamps. Accordingly, we calculate the activity level in WiFi bands. The activity level of white space bands is calculated solely based upon the spectrum analyzer measurements.

Figure 4.2 depicts a map of the available white space channels with markers where we performed measurements in North Texas. To be representative of a broad range of community types, we consider populations of approximately 25 times one another according to the 2010 U.S. Census, Millsap (500), Weatherford (25K), and Dallas (1.25 M). We have collected measurements at multiple types of locations in Dallas, including

a downtown area, a residential area, and a university campus. In Weatherford and Millsap, we monitor wireless activities in three locations for 45 continuous minutes on a weekday in downtown, residential, and non-residential areas. Then, we post-process the data to calculate the activity level of each band in each location. First, we parse the SNR from the data logs via Perl scripts. Second, we merge the data from the two platforms according to their respective time stamps and calculate the activity level of each band across these locations. The activity level is then included in our framework as input parameter.

4.3.2. Results and Analysis

In this subsection, we discuss our measurements results and leverage our MAPE framework to analyze the influence of white space channels across areas with different population densities. As an initial experiment, we perform a drive test from Dallas to Weatherford with cruise control set to 60 MPH while on the highway. The result of the in-field spectrum drive test is shown in Figure 4.3 according to the location and time of the measurement. The measured activity via RSSI of 450 MHz is high in downtown Dallas and Fort Worth but has less signal activity in the urban and rural area between these city centers. The low activity detected in the WiFi bands is due to the distance from the highway being typically larger than the propagation range of predominantly indoor wireless routers. Our initial in-field measurement matches the FCC restrictions (shown in Figure 4.2) with less channels available translating to greater spectrum utilization by TV stations. The drive test also shows that the spectrum utilization is roughly proportional to the population density in Figure 4.3. We use the measurements collected at more fixed locations as marked on the map for the activity level calculation.

The activity level calculated with our measurements are shown in Table 6.1. Dallas, the city with the greatest population in North Texas, has the highest activity level

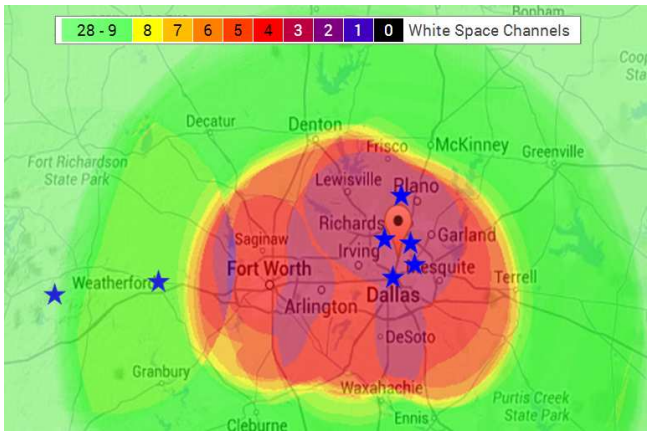

Figure 4.2: White Space Channels in DFW Metropolitan and Surrounding Areas.

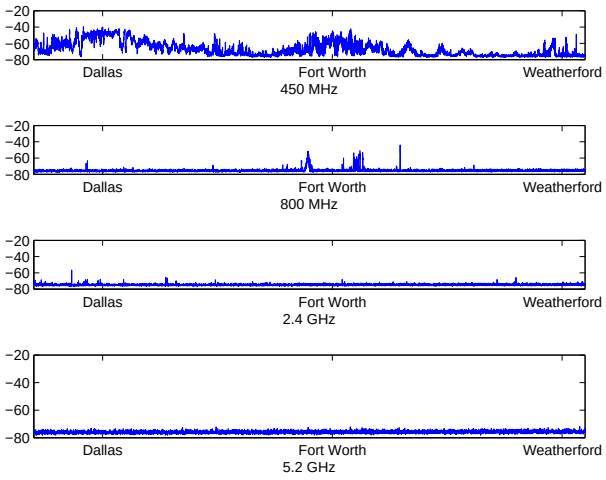

Figure 4.3: Spectrum Activity in DFW Metropolitan and Surrounding Areas.

Bands	Dallas			Weatherford		
Area Type	Downtown	Residential	Suburban	Downtown	Residential	Sparse
450 MHz	24.37	25.83	23.77	6.05	12.50	14.03
800 MHz	4.40	16.49	4.77	5.22	5.07	4.43
2.4 GHz	15.87	34.95	2.60	2.03	2.03	2.77
5.2 GHz	19.70	35.46	1.53	1.93	1.93	1.33

Table 4.1: Activity Level in Dallas & Weatherford

Bands	Millsap		
Area Type	Downtown	Residential	Sparse
450 MHz	7.00	0.07	0.02
800 MHz	3.87	4.20	3.60
2.4 GHz	2.07	1.60	0.80
5.2 GHz	1.27	2.07	2.10

Table 4.2: Activity Level in Millsap

in most of the measured bands, especially at 450 MHz. The Dallas urban measurements are taken from the SMU campus, two neighborhoods, and a densely-populated suburb (Plano). Our measurements indicate that 2.4 GHz has a higher activity level in urban area than the measured downtown area. Most schools and their neighborhoods are covered by WiFi, which contributes to the high activity level at 2.4 GHz and 5.2 GHz. In Weatherford, all the bands have lower activity levels than in Dallas. A peculiarity in the measurements can be seen by the sparse area in Weatherford having more activity than the other regions for 450 MHz. This can be explained due to the measurement location being on the East of Weatherford (closer to Fort Worth, which has a population of approximately 750k). Millsap is a typical sparse rural area with approximately 500 total residents. The activity levels across all the bands are lower than in Dallas and Weatherford. In the 450 MHz band, the activity level decreases much faster than in other bands in Dallas and Weatherford.

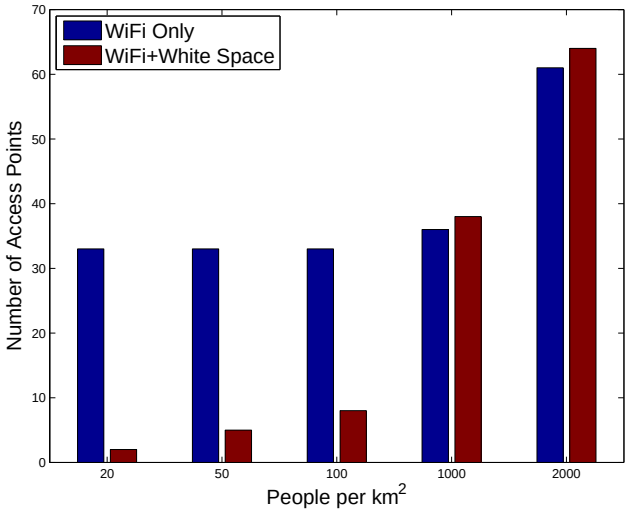

Figure 4.4: Number of Access Points Needed for a 13 km x13 km Area.

We use the measurement-based activity levels shown in Table 4.1 and 4.2 in our framework presented in Algorithm 4.1. We specifically use the Millsap sparse area, Millsap downtown, Weatherford residential, Dallas residential, and Dallas downtown measurements as inputs of activity level for a given population density. We then calculate the number of access points for covering a 13 km $\times$ 13 km area, varying the population density. The output is shown in Figure 4.4.

In the calculation, we set the demand requested per user as 2 Mbps with the population density of 20, 50, 100, 1000, and 2000 users per square kilometer. We assume 30 % of the residents will use this service (i.e., the take rate is 30 %), the maximum transmit power is 30 dBm, and a path loss exponent of 3.5 [58]. From Equation 2.1, we see that the propagation range is proportional to the wavelength with 450 MHz having a propagation range of 11.6 times that of 5.2 GHz. We adopt an 802.11n maximum data rate of 600 Mbps. For the WiFi+White Space scenario, we use 3 channels in each of the 450 MHz, 2.4 GHz and 5.2 GHz bands. For the WiFi Only scenario, we assume 6 channel in the 2.4-GHz band, and 3 channels in the 5.2-GHz band since 2.4 GHz has larger propagation range than 5.2 GHz. Each of these scenarios have the same channels in total (9). As shown in Figure 4.4, with the

same number of channels, WiFi+White Space reduces the number of access points by 1650% compared to the WiFi Only scenario in the 20 people per square km scenario, 660% in the 50 people per square km, and 412.5% in the 100 people per square km scenario. The large propagation range of the white space bands is approximately 10 times that of the WiFi bands, creating an opportunity for greater coverage. However, as the population density increases, due to the capacity constraint of servicing users in the area, the lower-frequency white space bands lose their advantage of larger communication range due to the reduction in achievable spatial reuse. At the same time, the activities of other signal sources, such as TV stations in downtown areas, reduce the capacity of white space bands. As a result, the WiFi+White Space scenario performs worse than the WiFi Only scenario. If we were to count the intra-network interference (out of scope), the situation could become even worse. Moreover, FCC has stricter policies on white spaces in urban areas. Fewer channels are available in these areas, which makes WiFi a better option for dense areas.

To understand the influence of band combinations on network deployments, we calculate the number of access points in the area when selecting 500 people per square km with a downtown Weatherford spectrum utilization and 1500 people per square km with a residential Dallas spectrum utilization. We assume the total number of channels is 12. We use the same setup as the previous experiment.

In Table 4.3, we compare the number of access points with 12 channels through all the possible combinations of bands. Since purchasing and deploying access points is the primary cost of a wireless infrastructure, to simplify the calculation, we only count the number of access points as the network's cost. When all the channels are in the same band, as the frequency goes up, more access points are needed to serve the area due to the limited propagation range. However, 450 MHz does not outperform 800 MHz with a single band at both the 500 and 1500 people per square km cases because

No. of Bands	Bands Combination (Hz)	No. of AP	
		500 ppl/km^2	1500 ppl/km^2
1	450 M	12	35
	800 M	10	30
	2.4 GHz	33	37
	5.2 G	193	193
2	450 M,800 M	11	32
	450 M,2.4 G	23	36
	450 M,5.2 G	23	69
	800 M,2.4 G	20	33
	800 M,5.2 G	20	59
	2.4 G,5.2 G	33	73
3	450 M,800 M,2.4 G	16	33
	450 M,800 M,5.2 G	16	48
	450 M,2.4 G,5.2 G	33	53
	800 M,2.4 G,5.2 G	30	49
4	450 M,800 M,2.4 G,5.2 G	21	44

Table 4.3: Channel Combinations for 500 and 1500 Population Density Scenarios

450 MHz channels have larger measured activity levels. White space band channels outperform WiFi bands by up to 1830% in the single band case with 500 people per square km, but with 1,500 people per square km, the cost reduction decreases to only 543%. We now distribute an equal number of channels to two-band combinations and run the experiments with the same population densities and spectrum utilization. The results shows the white space band combination (450 and 800 MHz) performs better than WiFi only (2.4 and 5.2 GHz) by 200% and 128% with the people per square km of 500 and 1,500, respectively. In fact, the white space only scenario (450 and 800 MHz) has almost the same performance as the scenarios with one white band and one WiFi band (450 MHz and 2.4 GHz; 800 MHz and 2.4 GHz) with 1,500 people per square km. However, with 500 people per square km, the white space only scenario

is much better than any other two-band combination. White space channels provide up to 87.5% cost reduction in three-band combination scenarios with 500 people per square km, and up to 33.3% with 1,500 people per square km. With four bands, the number of access points required does not reduce using white space bands.

From Figure 4.4 and Table 4.3, we show that as the population density increases, the reduction in number of access points required to meet the same demand diminishes. Note that a more optimal allocation of channels in different bands could offer further cost reductions. We further show that as population and spectrum utilization increase, at some point, the performance of white space only scenario could be the same as a combination of white space and WiFi bands.

4.4. Heterogeneous Access Point Band Selection

As opposed to previous works such as [31, 73, 80], these works focus on heterogeneous access point selection for wireless access networks which jointly employ WiFi and white space bands. We propose a relaxed linear program to find the lower bound of the number of access points and MHAPD algorithm to approach the lower bound number of access points which serve the traffic demand of a certain area. We assume the service provider has a limited number of spectrum resources and radios have similar configurations in terms of transmission power and bandwidth per channel use. Each radio on an access point operates with a classic protocol model as introduced in [37]. We further assume that there is a given take rate and traffic demand for a given population (as specified in Section 4.5).

Under the capacity and coverage constraints, the service area of a heterogeneous multiband access point deployments varies according to the traffic demand. The service area is limited by the propagation range when the traffic demand is low when the traffic demand is high, the service area is limited by the radio capacity. The

radius of the service area r_s could be represented as:

$$r_s = min\{r_p, r_c\} \tag{4.2}$$

Here, r_p represents the propagation range of a radio in the access point, and r_c is the capacity range of a a radio in the access point. When the traffic demand is distributed uniformly in a circle, from Eq. 4.1 the capacity range r_c could be noted as $r_c = \sqrt{k/\pi}$. Moreover, the propagation range and capacity range could be determined by the environment, traffic distribution, and transmission power control [73]. These factors are out of the scope of this work, but they could easily be added to the model for calculation of the heterogeneous access point service area. To simplify the problem and focus on the role of multiple frequency bands, we assume the traffic demand is uniformly distributed and the propagation follows Friis rule as Eq. 2.1. When the target area is given, we could obtain the service area of each access point type through 4.2, we then adjust the transmit power of each radio to reduce the interference.

When the traffic demand of an area is constant, the service area of a heterogeneous access point varies with the radios due to the constraints. We assume all the access points have the same number of radios and channel resources. In a low traffic demand scenario, the service radius reaches the radio propagation range. A high frequency WiFi radio will have a smaller service area since the signal attenuate faster; while the white space radio could have a larger service area due to the longer propagation range; and a heterogeneous access point who has both WiFi radios and white space radios has the same range of as low frequency radios access point. An example is shown in Fig. 4.5. In a medium traffic demand scenario, heterogeneous access points and white space access points will have the same size service area which is larger than high frequency WiFi only access points as shown in Fig. 4.6. With high traffic demand, all access points will have the same service area due to capacity constraint

as shown in Fig. 4.7. White space bands could reduce the cost of wireless network deployment due to greater inter node spacing. Thus, lowest cost for covering a certain area is to use white space bands in all access points it the traffic demand and user density is sufficient. However, spectrum resources are limited and the use of white space bands are restricted in major cities in the US due to TV channel occupancy [8]. Thus, the tradeoff between centralized use of white space bands or mixed use of white space bands and WiFi bands under multiple traffic demands is question for wireless network deployment. The problem could be modeled as how to use the minimum number of different sizes of service area according to radio combinations to cover a certain 2- D plane. This problem is a to deploy different size of cells in a given plane, which is a NP-hard bin packing problem [56]. We propose a relaxed linear program to achieve the lower bound of the number of access points and a heuristic algorithm to approach the lower bound.

Given a target area G with the traffic demand distribution γ, the service area of all kinds access points S_t, and the coverage rate p, the capacity of access point C_t could be calculated based on the number of radios, Friis model in Eq. 2.1 and restriction constraints in Eq. 4.2 or from in-field measurement [24]. When the target area is served, the reward of the area could be calculated as R. However, the reward of service carrier does not influence the optimal deployment since the total reward is a constant when the user number is constant in the service area in our scenario. Furthermore, the minimum number of access points could be found through a relaxed linear program as follows.

Sets:
B Set of Bands
T Type of Access Point

Parameters:

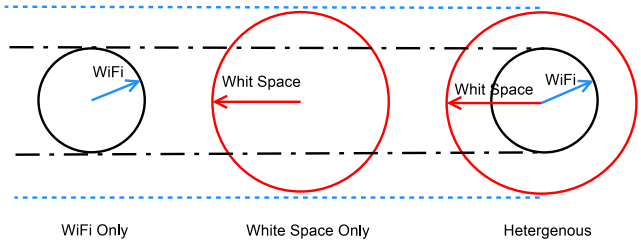

Figure 4.5: Low Traffic Scenario

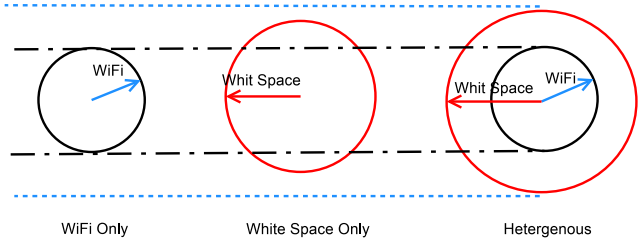

Figure 4.6: Medium Traffic Scenario

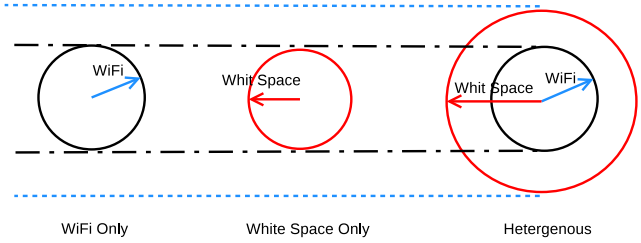

Figure 4.7: High Traffic Scenario

G		Target Area
γ		Traffic Demand Distribution
p		Coverage Rate
S_t	$t \in T$	Coverage Area of Type t AP
$O_{b,t}$	$b \in B, t \in T$ *binary*	Channel Occupied by Type t AP
N_b	$b \in B$	Available channel of a band in Target Area
C_t	$t \in T$	Channel capacity of Type t AP

Variables:

$a_t \geq 0 \quad t \in T \quad$ Number of Type t AP

Objective:

$$Min \sum_t a_t \tag{4.3}$$

Coverage Constraint:

$$\sum_t a_t \cdot S_t \geq G * p \tag{4.4}$$

Capacity Constraint:

$$\sum_t a_t \cdot C_t \geq G \cdot \gamma \tag{4.5}$$

Resource Constraint:

$$\sum_t a_t \cdot O_{b,t} \leq N_b \tag{4.6}$$

Spatial Constraint:

$$a_t < \frac{G}{S_t} \cdot \frac{2}{3} \cdot N_b \tag{4.7}$$

The linear program relaxes the coverage constraint without providing a key parameter where the access points are located. Moreover, the linear program may provide multiple results since different types of access points could have the same service area,

(e.g. in a low traffic demand case) The result of the linear program is the lower bound on the number of access points.

In order to find a practical access points deployment in multiband scenario, we represent a greedy local search algorithm in Alg. 4.2. The service area of access points varies across diverse population distributions. Assume the cost of building an access point is the same as C_a. When an access point is built, the more service area the better. Thus, heterogeneous access points could always have better performance. However, since there are a limited spectrum resources, we have to balance the usability of heterogeneous access points which reduce the cost of building a network, and single radio access point which may cover more area.

In the linear program, the reward R is a constant of the area G. But for a single heterogeneous access point deployment, we have to compare its reward and cost to separately using the radios. In a certain area, a heterogeneous AP has radius r_1. If we separately use the radios with radius $r_2, r_3, \ldots r_n$, the reward is uniformly distributed and the heterogeneous reward is defined as:

$$H_r = (n-1)C_a - \frac{R}{G} \cdot \sum f_s(r_n) \tag{4.8}$$

Here, $f_s(r)$ is the area calculated function, for example, $f_s = \frac{3\sqrt{3}}{2}r^2$ when a hexagonal coverage model is applied. In the framework, the access point type with greater reward is going to deployed first until the available resources are used up. When two types of access points share the same unit price, considering the spatial reuse, the access points with high frequency channels will be chosen. The deployment starts from the edge of the given plane and we use a protocol model to find the available access point types. If the combination of a unit grid could be covered by an access point, we put the unit grid in the coverage area until the access point can not access any more of grid. Then we switch to another available access point. The process is

like a Teris game, when a given access point is filled, it will be deleted.

Generally, we employ access points with larger coverage capacity to fill in the area. Then through the algorithm, we could cover the target area by the most efficient access point type, step by step until a minimum number of access points and a practical multiband wireless deployment is achieved.

4.5. Numerical Evaluation and Analysis

To evaluate the performance of heterogeneous wireless network deployment, we perform numerical evaluation with linear program, and MHAPD algorithm to analyze the role of white space and WiFi bands in total access points required for a given deployment area.

4.5.1. Experimental Setup

In the evaluation, we set the demand request as 2 Mbps per person with the population density from 20 to 2000 per square kilometer. We assume 30% residents will use this service, the maximum transmit power is 30 dBm, and a path loss exponent of 3.5 from Ref. [58].

We adopt an 802.11n maximum data rate of 600 Mbps. In the protocol model, the interference range is as twice as the communication range. We investigate both traffic demand and the number of white space channel influence on heterogeneous wireless network deployment. We have interference free scenario, each band has at least 3 channels, which fits for most rural areas and some cities, such as Houston [7]. In this scenario, it is possible to use all heterogeneous access points since heterogeneous access point could serve more area. However, in the field, there are some cities has area only one or two licensed white space channel, such as Salt Lake City [7]. In these scenario, only part of the access points could be heterogeneous. We run numerical

Algorithm 4.2 Multiband Heterogeneous AP Deployment

Input:

G: Target Area

R: Reward of Target Area

γ: Traffic Demand Distribution

p: Coverage Rate

S_t: Coverage Area of Type t AP

$O_{b,t}$: Channel Occupied by t Type AP

N_b: Available channels of a Band in Target Area

C_t: Channel Capacity of Type t AP

1: **while** $\sum A \cdot S_t < p$ **do**

2: Rank available AP type according to their unit price H_r

3: Rank available AP type according to radio numbers

4: **if** The reminder area G_r is larger than all the available AP **then**

5: Choose the AP has the largest coverage area S_t

6: **else**

7: Find the available AP type whose coverage area $S_t = minS_t > G_r$

8: **end if**

9: Deploy an AP at the left up edge of un-covered area

10: Fill the AP with one neighbor unit grid and move the AP in the center of the coverage area

11: Update Channel Resource $O_{b,t}, N_b$

12: Update Output Access Point A

13: **end while**

Output:

The number of Access Points and Deployment

simulation of both the scenarios and analyze the heterogeneous access points amount of the results.

We given the target area as 15×15 square kilometers. In the numerical simulation, we assign orthogonal WiFi channels in 2.4 GHz,5.8 GHz and white space channels in 450 MHz, 800MHz. Then we calculate the service area of access point according to their radio combinations as described in 6.1.2 with a hexagonal model. Then we run our linear program and MHAPD methods to investigate the benefit from white space band and in what degree heterogeneous access point is beater than single radio access point.

4.5.2. Results and Analysis

Fig. 4.8 shows access point number to serve the target area when the area has more than 3 white space channels, which means white space radios could be used on all access points in hexagonal deployment model. In the simulation, we set 3 white space channels in 450 MHz. In this scenario, at the beginning, the served area of WiFi only access point is restricted by the communication range. As the population distribution increase, the served area of WiFi only access point will be limited by the traffic demand instead of the communication range. The curve keeps flat until the traffic demand becomes the limitation of the served area. In the heterogeneous deployment, the served area is restricted by the traffic demand at the beginning, the number of access point increase as the traffic demand increase. Also since there are enough channels can be reused, our algorithm use almost the same number of access point to serve the target area. In this scenario, as population distribution increase, the gain of adding white space channels in our algorithm comparing with WiFi only(2.4 GHz) decrease from 686% to 248% and keep around the value 260%. The gain is from the large propagation range of white space bands at low population distribution. As the population distribution increase, which means the traffic demand increase, some

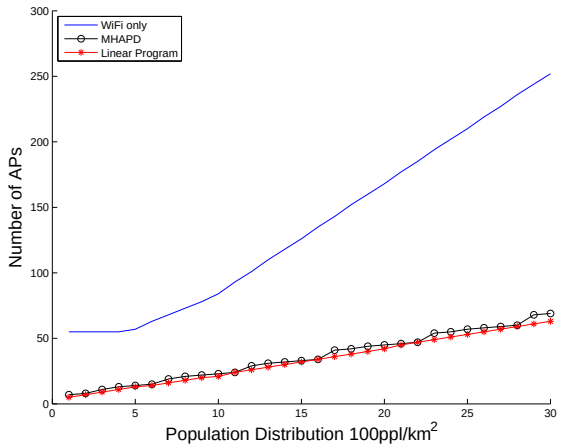

Figure 4.8: Sufficient White Space Channels Scenario

of the gain comes from more capacity of heterogeneous access point.

With few white space band Chane's(less than 3 channels), in the hexagonal model, only one or two neighbor access point could use white space channel. Fig. 4.9 shows the simulation result of one 450 MHz channel deployment. Shortage of white space channels make the number of access points much more than the linear program calculation. The gain from white space channel is from 323% to 86%.

In these sufficient and shortage of white space channel scenarios, the highest gains are from low population distribution. This result represent that white space band fits rural or suburban area where has few residents. When the population distribution increase, the benefit of white space channels is from their bandwidth, which is the same as adding more WiFi channels.

In Fig. 4.10, we investigate the percentage of heterogeneous access points in 3 white space channels scenario and two white space channels scenario in our algorithm. With sufficient white space channels, we prefer heterogeneous access point and there is no limitation of the heterogeneous access point deployment. The percentage of heterogeneous access points is higher than 80%. In two white space channels scenario, at the beginning the number of hetergeneous access point is restricted by the interfer-

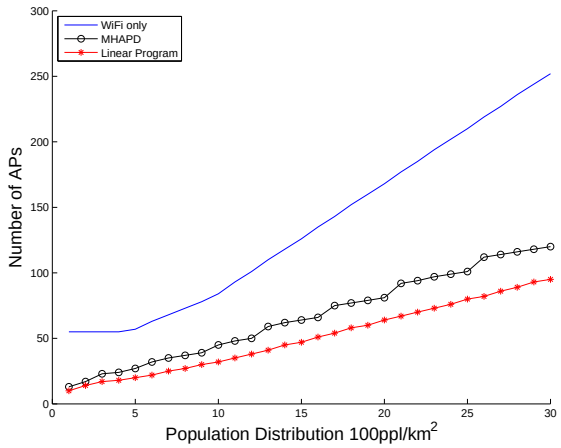

Figure 4.9: One white channel

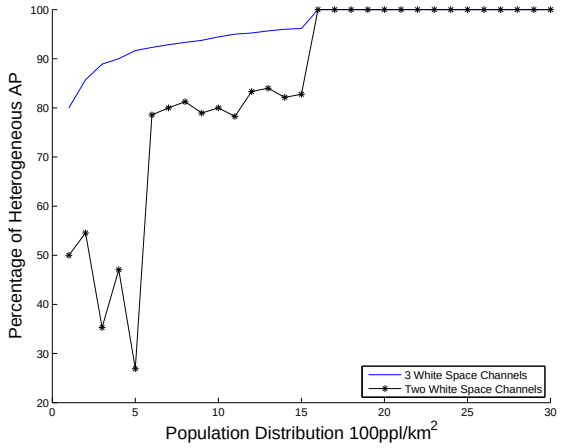

Figure 4.10: Percentage of Heterogeneous Access Points

ence range. As the population increase, no more heterogeneous access point could be added in the target area, we have to add more WiFi access point which makes the heterogeneous points percentage decrease. When the population distribution reach the threshold which the traffic demand restrict the service area of heterogeneous access point, the percentage increases. When the service area shrink as the WiFi access point, since they have more capacity, all the access points become heterogeneous. In the white space channel shortage scenario, white space channel becomes the inside service area of heterogeneous access point to explore spatial reuse.

As shown in the numerical simulation, the heterogeneous access point could balance the spatial reuse and large service area to adapt multiple traffic demand scenarios. The combination of white space bands and WiFi bands could reduce the cost for network deployment significantly.

4.6. Summary

In this chapter, we jointly considered the use of WiFi and white space bands for deploying wireless access networks across a broad range of population densities. To consider network deployment costs, we proposed a Multiband Access Point Estimation framework to find the number of access points required in a given region. We then performed spectrum utilization measurements in the DFW metropolitan and surrounding areas to drive our framework and find the influence of white spaces on network costs in these representative areas. Through extensive analysis across varying population density and channel combinations across bands, we show that white space bands can reduce the number of access points by 1650% and 660% in rural and sparse urban areas, respectively. However, the same cost savings are not achieved in dense urban and downtown type area. Finally, we investigate different band combinations in two population densities to show that greater access to white space channels have greater total savings of mesh nodes when the total number of channels used in the network is fixed (i.e., given a total number of allowable WiFi and white space channels). As the population and spectrum utilization increase, the cost savings of white space bands diminish to the point that WiFi-only channel combinations can be optimal. Through extensive analysis across varying population density and channel combinations across bands, we show that white space bands application in hetergeneous access point can reduce the number of access points by 260% in sufficient white space configuration and 80% gain in limited white channel scenarios.

Chapter 5

Spectrum Adaptation for Scant White Space Resource

In this chapter, we study the white space resource impacts on mesh network power consumption via queuing theory model. We describe the heterogeneous wireless network structure with both white space bands and WiFi bands. We formulate the system as a queuing model. We analyze the heterogeneous structure under the the waiting time constraint for resource allocation in multiple scenarios of the structure. We further propose a Greedy Server-side Replace (GSR) algorithm to minimize the power consumption for the heterogeneous network structure. We then evaluate the algorithm, showing the power consumption gains across sparse and dense areas and analyze the impact of the number of white space and WiFi channels in these representative scenarios.

5.1. System, Assumptions and Problem Formulation

5.1.1. System and Assumptions

The propagation range of low frequency white space channels is times of WiFi channels, for instance, 450 MHz channels has more than 12 times propagation range as 5 GHz channels via Friis model. Thus a single white space access point is possible to serve an area up to hundreds times of a WiFi access point. The larger propagation of white space channels is potentially to be applied for reduction of network deployment cost [64], adaptation of vehicular dynamic access [21], and improvement of network capacity [15]. However, previous works focus on the application of plenty white space

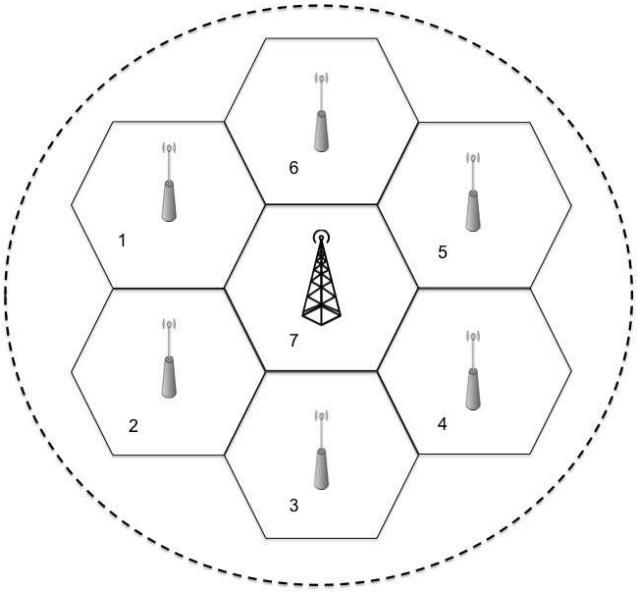

Figure 5.1: Heterogeneous WhiteCell Structure

channels resource or point to point communication require small amount of white space resource.

City	New York	Log Angeles	San Francisco	Seattle	Houston	Austin	D
White space channels	0	0	2	7	3	1	

Table 5.1: Number of White Space Channels in Major Cities

In wireless network design, as discuss in previous works, the more wireless channel resource means the better performance. Unfortunately, FCC restricts the number of white space channels in most dense populated areas due to the existing TV broadcasting application. The minimum number of white space channels in major cities in the U.S is listed in Table 5.1. There are areas has no white space channel available in New York and Los Angeles. Austin has only one white space channel available in downtown area. The other cities in the table have 2 to 7 white space channels. Thus, a heterogeneous network with WiFi channels and few white space channels becomes a practical option for these cities other than a white space wireless network.

Here, we introduce a heterogeneous network named as WhiteCell with existing WiFi cells and an access point with few number of white space channels as shown in Fig. 5.1. Given a WiFi mesh wireless system with M access points and N users. The users in each WiFi cell of the network have access to the white space channels and the assigned WiFi channel of the cell. The reuse of WiFi channels has been discussed in plenty of previous works and it is out of our scope. There are F_w white space radios is installed on one of the access points to assistant the existing WiFi network. The capacity in clean environment of each radio C is an equally restrict number for all the channels. There are enough buffer store the traffic demand from the users on each radio. The traffic is served in a first-in-first-out (FIFO) scheduling system. In such a network, each user has $1 + F_w$ channels to be scheduled. One is the previous in-cell WiFi channel and the white space channels. We assume the users in the same mesh cell are in a single interference domain. Considering the limited number of white space channels in dense area and the fact spatial reuse of white space will make the problem considerably more challenging, we will remains an interesting direction of future research.

Instead of assuming the wireless channels are on-off [18] or equally clean, we apply a measurement method to get the achieved channel capacity. The capacity of the channel between the access points and users is noted as a matrix in Eq. 5.1

$$H_{i,j}^{f}(t) = G(\zeta, t), i \in M, j \in N, f \in (F_M + F_w) \tag{5.1}$$

ζ represents the in-field measured historical data and dynamic sensing information. We use a context-aware method to estimate the j user capacity $H_{i,j}^{f}(t)$ to an access point i on channel f. The users in a single cell has the same channel status. We assume the channel capacity is flat during a time slot. The switching time is negligible in the system. The calculation of achieved channel capacity is introduced in 5.2.2. The traffic demand arrive at a user as a Poisson process, with the vector noted as

$\boldsymbol{D(t)} = [D_1(t), D_2(t), ...D_N(t)]$ and the sum rate $D(t) = \sum_{i=1}^{N} D_i(t)$. The rate $D(t)$ is the aggregate rate of data generated from all users.

During a time slot, the unscheduled radios remain in sleep mode to save energy. Also we ignore the sleeping energy as well as the amount of energy spent on channel/radio switching. An operating radio will cost equal power in a time unit. Previous work [62] shows a user has a certain patience for waiting. The tolerance time varies across the traffic type, such as text information, voice information. To simply the problem, we assume an average value for W of all the users in the system. The smaller tolerance time of the users, the more channel capacity resource is required. The system applies a first-come-first-serve schedule. The white space channels are able to split for multiple cells.

5.1.2. Problem Formulation

We formulate the system introduced in 5.1.1 as a discrete-time queuing system as shown in Fig. 5.2. The channels are represented as servers in the queuing system. Table. **??** summarizes the notation used in this work. The system has F_w white space channels, F_M WiFi channels in total and N users. Thus, the queuing system has N queues and $F_M + F_w$ servers connecting by time-varying channels $H^*(N, F_M + F_w)$.

Let matrix $\{A_{i,j}(t), i \in (F_M + F_w), j \in N\}$ denote the associate meets the tolerance constraint as shown in Eq. 5.2.

$$A_{i,j}(t) = \begin{cases} 1 & if\ D_{j \in N},\ is\ associated\ with \\ & channel\ i \in (F_M + F_w) \\ 0 & Otherwise \end{cases} \tag{5.2}$$

The queuing system keeps the expected waiting time of the system w less than the tolerance threshold W as shown in Eq. 5.3

$$E[w] \leq W \tag{5.3}$$

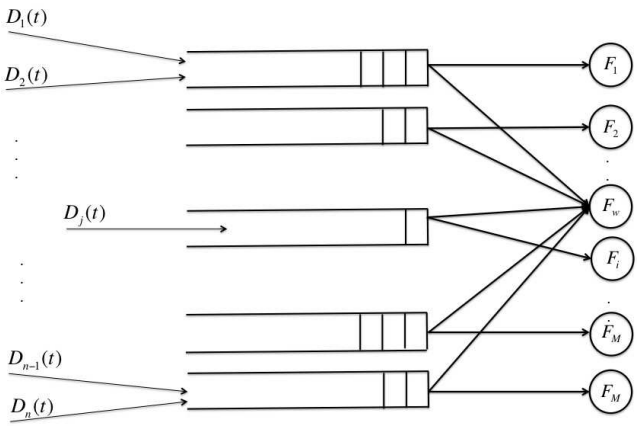

Figure 5.2: System Model

With the intuition, when the total traffic demand of the users in the system are relatively small, a single white space channel could achieve the quality of service for the users. Thus all the WiFi radios could be turned into sleep mode for power saving. On the other side, as the traffic demand increase with the number of users or the demand per user, we need to increase the channel resource as servers in the system to qualify the user waiting time tolerance requirements. Moreover, when the users are distributed non-uniformly, the white space channels are able to deliver more capacity for the cells with more users to balance the system load without new infrastructure. The flexibility of white space channels offers new opportunity for network design. To apply these white space advantages, the question *how much power we could save via dividing the white space capacity into the WiFi cells?* has to be addressed in this system.

In this work, we focus on the analysis on the power consumption saving of the heterogeneous wireless system. To model the power consumption of the system, we count the power consumption of each operating radio via standby and transmitting power consumption. We assume the sleeping standby power consumption is negligible. We define R_i represents the radios status in the system, $i \in F_w, F_M$. When R_i is working in WiFi channels F_M or white space channels F_w, R_i denotes the power

consumption with the standby and transmitting cost. Otherwise, $R_i = 0$. The definition is as shown in Eq. 5.4

$$R_i(t) = \begin{cases} P_s + P_t \cdot \mu & \sum_{j=1}^{N} A_{i,j}(t) \geq 1 \\ 0 & Otherwise \end{cases} \tag{5.4}$$

P_s is the constant standby power consumption of a radio, P_t is the transmit power for the channel capacity assigned of the radio. μ is the total assigned channel capacity of the radio. $R_i(t)$ is the power consumption of the radio in the time slot.

Thus, to reduce the power consumption, we need to minimize R_i for all the radios under the quality of service constraints. Our goal, to minimize the power consumption is represented in Eq. 5.5:

$$R^*(t) = \min\{ \sum_{i=1}^{(F_M+F_w)} R_i(t)\} \tag{5.5}$$

R^* represent the minimum operating radios power consumption required for the system.

5.1.3. Challenges And Analysis

Prior works formulate similar multi-channel system as $M/M/m$ queuing system for analyzing [18]. However, this system is not able to be formulated as a $M/M/m$ queuing system due to the non-equal capacity of the assigned channel capacity across white space and WiFi channels. Thus we first analyze the queuing system and apply previous work in $M/M/m$ queuing theory to generate the solution for such system.

Without the white space channels, the users in a cell can only access to the WiFi channel assigned for the cell to get service. The large propagation of white space channels offers more options for all the users. The user could either associate with the white space channels or the WiFi channels. Thus, the white space channels could be slitted into several cells. The splitting of the white space channels brings more

capacity variation of the servers. The white space channel splitting capacity variation and the spectrum capacity variation of cells might remove the equal service capacity assumption of the system in most scenarios. However, the equal server capacity is the pre-request for a general $M/M/m$ queuing system analysis. Thus, the $M/M/m$ queuing system of a multi-channel version is not directly applicable for this system model.

In the design of the wireless system, the response time W constraints have to be satisfied to keep the quality of service. The users in this system can only be served by the large propagate white space channels or the WiFi channels assigned in the cell. The users located in multiple cells have different channel status in the same white space channels, which is mentioned as part of the multi-user diversity in previous works. Multi-user diversity is a form of diversity inherent in a wireless network, provided by independent time-varying channels across the different users [85]. The diversity could be generated by the interference from device inside the network or out of the network, the environmental variations. The variation among users make the channel capacity among all the cells for white space channels. Thus, some cells may have clean white space channels in the air while the other cells may suffer worse white space channel performance. To address the variation, instead of holding the on-off channel assumption, we implement an in-field measurements based channel capacity estimation approach in this work.

We define an activity level to estimate the achieved channel capacity. We perform measurements to sense the activities in the air through our portable spectrum analyzer. The percentage of sensing samples (S_θ) above an interference threshold (θ) over the total samples (S) in a time unit is the activity level (A):

$$A = \frac{S_\theta}{S_a} \tag{5.6}$$

The capacity of a clean channel is denoted by C. With the protocol model, the achieved capacity of a channel C_r could be represented as the remaining free time of the channel capacity according to Eq. 5.7:

$$C_r = C * (1 - \bar{A}) \tag{5.7}$$

Other than the achieved channel capacity, we also perform in-field measurements of the user mobility footprint. When the total number of the users is a certain value, the user distribution becomes important for wireless network operating. We analyze the data set from WiEye, an Android application reports the location, velocity and signal information to leverage the mobility pattern of users during week days. The setup and results are shown in Section **??**.

With these measurements information, we further analyze the channel capacity allocation for such a system. We first investigate the channel capacity allocation in a single cell. The users of the the same WiFi cell are in a heterogeneous queuing system with server of WiFi channels and white space channels with service rate $\mu_1, \mu_2, ...\mu_{(F_w+1)}$. μ denote the capacity allocated for this cell. The white space channel capacity is slitted into multiple WiFi cells, thus, the capacity of the white space is usually the minimum channel capacity in a cell. Thus, there are three cases of the channel capacity in a single cell. The first scenario is several channels of both WiFi and white space works for the cell and the capacity of some white space channel is several time less than other channel capacity since white space channels are slitted for many cells. An example here is in a single cell, the white space channel assigned is equally distributed to two cells, while the WiFi channel works in this cell, thus, the capacity of the WiFi channel is about twice of the white space channel capacity in this cell. The second scenario is only the WiFi channel or only part of a single white space channel works for the cell. The third scenario is several channels work for this cell with around equal capacity. The fist case is a heterogeneous server queuing

system with unequal capacity servers. The second case is simplified as a $M/M/1$ queuing system. The third case is converted into a $M/M/m$ queuing system.

For the first case heterogeneous server queuing system, we apply the transformation model in [89] to estimate the response time $\bar{w}$. In the transformation model, the actual arrival rate for one specific server λ_s is defined as in Eq. 5.8

$$\lambda_s = D_{cell}/(F_w + 1) \tag{5.8}$$

D_{cell} is the traffic aggregated from the users in the cell.

The other parameters are noted from Eq. 5.9 to 5.11.

$$\mu_{min} = \min(\mu_1, \mu_2, ...\mu_{(F_w+1)}) = \bar{\mu} \tag{5.9}$$

$$\mu_{max} = \max(\mu_1, \mu_2, ...\mu_{(F_w+1)}) \tag{5.10}$$

$$k = \lfloor \frac{\mu_{max}}{\mu_{min}} \rfloor \tag{5.11}$$

When $k = 1$, the system becomes a homogeneous queuing system as in case three. Otherwise, $k \geq 2$ the average response time of such heterogeneous system [89] could be represented as in Eq. 5.12:

$$\bar{w} = \frac{1}{\frac{1}{3}\bar{\mu}(2k+1) - \lambda_s} \tag{5.12}$$

Through the transformation model, we could further calculate the channel capacity required for response time constraints. Further, the power consumption could be calculated for the system. When the traffic could be served by part of a single white space channel or the WiFi channel, as the second scenario, the system converge into a $M/M/1$ queue. The response time $\bar{w}$ could be estimated from Eq. 5.13 [33].

$$\bar{w} = \frac{1}{\mu^+ - D} \tag{5.13}$$

μ^+ is the channel capacity of the single channel capacity in queuing system.

In the third scenario, the system could be treated as a $M/M/m$ queuing system. The average response time is calculated as in Eq. 5.14 [33].

$$\bar{w} = \frac{1}{\mu^*}(1 + \frac{c(m,\rho)}{m(1-\rho)}) \approx \frac{1}{\mu^*}\frac{1}{1-\rho^m} \tag{5.14}$$

μ^* is the average capacity of channels in the $M/M/m$ queuing system. $\rho = \frac{\lambda}{m\mu^*}$ is the traffic density, and $c(m,\rho)$ is the Erlang-C formula [33].

In this model, the less radio in operation and the less power consumption will be cost in the system according to Eq. 5.4. The basic idea of power reduction for this heterogeneous system is to replace the WiFi radios via white space channel capacity. To implement the division of the white space capacity we propose a Greedy Server-side Replace(GSR) algorithm to approach the minimize power consumption in the system as shown in Algorithm 5.1.

The algorithm input the measurement-based achieved channel capacity, the number of white space channels and the WiFi cells. The white space channels are employed for the cell with less traffic demand to reduce the standby power. The algorithm compare the three configurations of channel capacity and tell the setup with the best power consumption. Further, the process is repeat till all the traffic demand are served or the channel resource has been used up. Then output the power consumption and channel allocation of the system.

5.2. Experiment and Analysis

In this section, we introduce the in-field measurements experiments , the evaluation of the heterogeneous wireless system and analysis of the results.

5.2.1. In-field Measurements

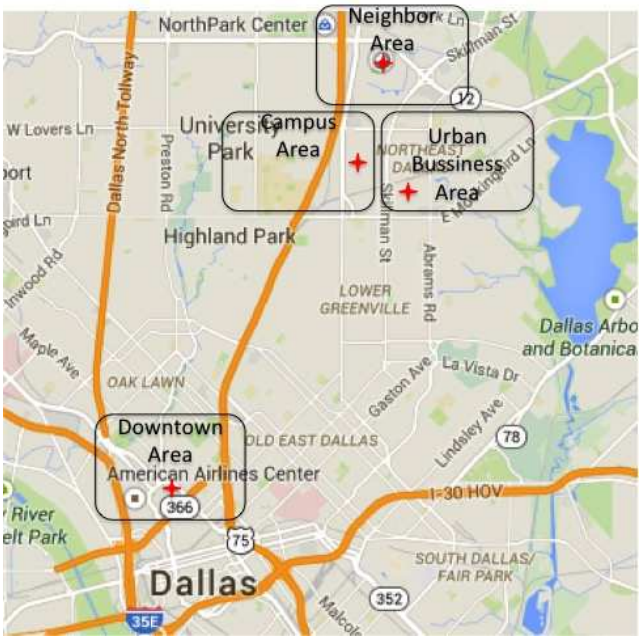

Figure 5.3: Long Term Measurements Locations

We perform in-field measurements in typical areas to find the channel state variation across time and the user mobility patterns among the areas. We chose neighborhoods, campus, downtown business office and urban business office to perform long term 24 hours measurements on weekdays. The locations we chosen are located in Downtown Dallas, a university campus in Dallas, a business in Dallas urban area and an apartment on north Dallas. The locations where we collected measurements are shown in Fig. 5.3.

In each of the location, we left our equipment running to measure the channel state for 24 hours during weekdays. We employ a Rohde & Schwarz FSH8 portable spectrum works from 100 KHz to 8 GHz. The portable spectrum analyzer is controlled by a Python script on a laptop to measure the received signal strength. To the best of our knowledge, there is no readily available mobile, multiband antenna from 450 MHz to 5.2 GHz on the market. Thus, we use a 700-MHz mobile antenna to perform in-field measurements. We then normalize the mobile antenna performance across bands

with indoor experimentation. To do so, we use a Universal Software Radio Peripheral (USRP) N210 to generate signals at 450 MHz, 800 MHz, and 2.4 GHz. We feed the USRP signals directly to a spectrum analyzer and adjust the configuration of USRP to make the received signal strength the same as the 5.2 GHz signal from Gateworks 2358 with a XR5 radio. Then, we connect the signal source to a fixed multiband antenna (QT 400 Quad Ridge Horn Antenna) and measure the received signal at a fixed distance with the 700 MHz antenna and antennas for different bands to obtain the antenna loss for each band. We adjust the received signal strength collected via the 700-MHz mobile antenna according to the normalization. We use $-85dBm$ as a threshold in the activity level calculation for the normalized data.

When wireless devices operate in WiFi bands, the channel separation is relatively small (e.g., 5 MHz for the 2.4 GHz band). As a result, many works assume that the propagation characteristics across channels are similar. However, with the large frequency differences between WiFi and white space bands (e.g., multiple GHz), propagation becomes a key factor in the deployment of wireless networks with both bands. Here, a frequency band is defined as a group of channels which have little frequency separation, meaning they have similar propagation characteristics. In this work, we consider the diverse propagation and activity characteristics for four total frequency bands: 450 MHz, 800 MHz, 2.4 GHz, and 5.2 GHz. We refer to the two former frequency bands as white space bands and the two latter frequency bands as WiFi bands. The differences in propagation and spectrum utilization create opportunities for the joint use of white space and WiFi bands in wireless access networks according to the environmental characteristics (e.g., urban or rural and downtown or residential) of the deployment location.

Through the measured data set, we calculate the activity level via Eq. 5.6. The activity level is calculated in one minute time window. We average the activity level

Downtown 450 MHz	0:00-11:00	22.09	21.27	22.28	22.47	21.65	21.68	22.37	22.1
	12:00-23:00	21.80	20.86	21.80	22.54	22.35	22.61	22.45	21.5
Campus 450 MHz	0:00-11:00	20.29	21.56	21.41	22.52	23.12	21.97	21.65	21.6
	12:00-23:00	22.33	22.88	22.28	21.65	22.49	22.16	21.32	22.3
Neighborhoods 800 MHz	0:00-11:00	15.72	16.30	16.33	15.72	16.54	14.48	14.62	14.4
	12:00-23:00	15.72	14.74	14.74	14.38	15.41	15.00	15.84	16.2

Table 5.2: Part of Activity Level in Multiple Locations
in 30 minutes across 24 hours.

Through the activity level results, we observe that the activities of 450 MHz in the air has almost the same patterns across all the four measured areas. The large propagation area of 450 MHz influence the areas simultaneous and the 450 MHz activities are perform regularly on weekdays. Neighborhood area has more activity in 800 MHz than other types of areas. But the 800 MHz activity levels are relatively lower than other bands in all the areas. The WiFi 2.4 GHz channel of neighborhoods has more activity in the night while the downtown area has more activity in the day time. The campus has more WiFi activities in the morning than the afternoon and night. Part of the measurements results are list in Table 6.1. Due to the limited space, the full list of measurements are available upon request. We integrate the measurements result into our numerical simulation of GSR algorithm later in this section.

We choose the data from WiEye database according to the GPS location. The data we chosen from Dallas area, including downtown, urban, SMU campus and neighborhood area. We note the SMU campus area size as the unit, find the same size of downtown area and urban area. The rest of the chosen locations are counted as neighborhoods. The size of neighborhoods area is about 2.8 of campus area. The data set is generated from Oct. 1st 2014 to March 20th 2015. We track the identified 538 users from the data set in different types of areas. The number of users located in these area are counted according to the GPS and further converted into the percentage

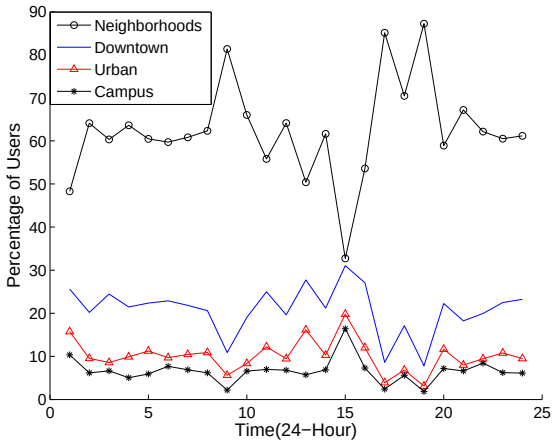

Figure 5.4: User Distribution across Time

each hour. The percentage distribution of users across these areas during a weekday is shown in Fig. 5.4

From the measurements results, we could find the distribution increase from 9:00 AM in the morning till 3:00 PM in the afternoon in downtown, urban business area and campus. This match the most of the work schedule. The peak of neighborhoods is around 6:00 PM in the afternoon and 9:00 AM in the morning. The reason could be the users are looking for breakfast in the morning before go to work. We input the user mobility pattern into our power consumption numerical simulation.

5.2.2. Experiments, Results and Analysis

We apply our GSR algorithm with the measurements in a virtual city to investigate white space band impacts on power consumption. The virtual city in our experiment includes a downtown area, a school campus area, two urban business areas and three neighborhood areas. All the areas are in the same size with a single WiFi cell. The white space channels has more than 3 times propagation range than WiFi channels even with the lowest frequency WiFi channel and the highest white space channel. The white space radios are located in the center of the virtual city cover all the users

in the four types of areas. We assume the residents in the city is a constant number which could be calculated through the population distribution according to the 2010 U.S. Census [9]. The channel variation of spectrum is setup according to the channel state measurements and the user mobility from the measurements results of WiEye introduced in Subsection 5.2.1.

The transmit power of radios are equal and with the same clean channel capacity. The standby power consumption of a radio is 500 watt and transmit power is 1 watt per Mbps. We lookup population distribution from the US census 2010 to calculate the users in the virtual city. We set the demand requested per user as 0.5 Mbps and assume 30% of the users will activate their device (ie. the take rate is 30). The tolerance time of users is 30 ms in most of the simulations. We adopt an 802.11n maximum data rate of 600 Mbps for all the radios. For the single white space channel setup, the channel is from the 800 MHz. For two white space channels, one is 450 MHz, the other one is from 800 MHz. For three white space channels setup, two of them are from 800 MHz and one from 450 MHz.

We first investigate the power consumption variation across time with the population distribution as $2000 ppl/km^2$ with the measurements setup. The results across 24 hours of the virtual city is shown in Fig. 5.5

We observe that the WiFi power consumption keeps constant in most case. That because the WiFi propagation range restrict all the radios have to be on operating to serve the users. While the white space radios could adapt the user non-uniform distribution or user mobility better. When the user distribution changes fast at 9:00 AM, the white space configurations could reduce the power consumption by about 20% of the previous user distribution. Three white space channels could reduce almost half of the power consumption in the simulation. The power consumption gain is mainly from turning off the radios. When the users are uniform distributed,

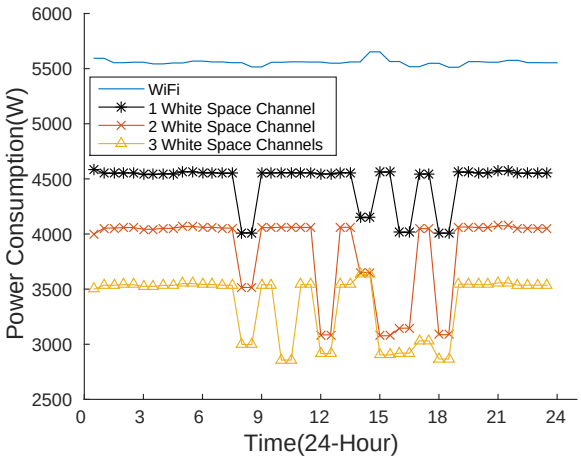

Figure 5.5: Power Consumption across Time

the power consumption may increase due to the splitting of white space channels. The queuing theory concludes that a single faster server is better than multiple slower server have the same capacity. When the users are uniform like distributed, the white space channels may be divided into several sub-channels which lower the performance. From the measurements numerical simulation, one white space channel could reduce the power consumption by 24.57% during 24 hours. Two white space channels could reduce by 46.27% and three white space channels could reduce by 67.40% relatively. As the number of white space channel increase, the power consumption gains per channel will become a constant since there is enough channel capacity to satisfy the users. Thus, according to the result, we could design the network with white space channels to adapt the user mobility patterns with affordable power consumption as well as apply the white space channels as complement resource for the existing WiFi infrastructure.

Further, we study the tolerance waiting time W of users impacts on the power consumption. We keep the population distribution as 2000 ppl/km^2 and 11:00 AM channel state and user distribution. The tolerance waiting time is set from 5 ms to 90 ms with 5 ms steps. The results are shown in Fig. 5.6.

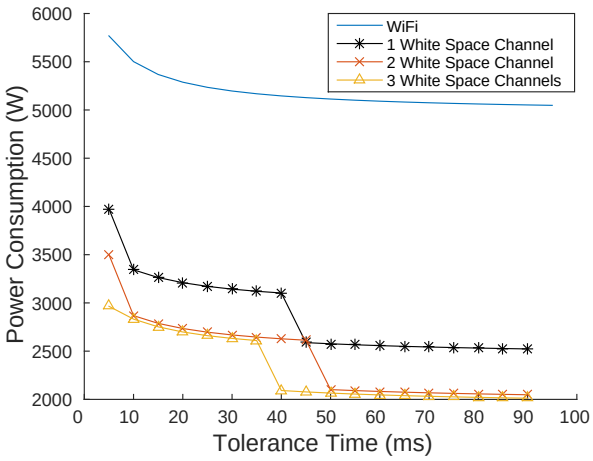

Figure 5.6: Power Consumption across Delay Tolerance

The results that the less quality of service in waiting time, the less power consumption is required. As the tolerance waiting time increase, the power consumption of both WiFi and heterogeneous configuration gains power saving. The WiFi configuration gains the power saving mainly from the reduction of channel capacity delivery. The white space configuration gains the power saving from both the reduction of channel capacity delivery and the sleeping radios. Thus, there are some sharp reduction in the white space setup in the numerical simulation results due to the radio turning off. The power consumption could be reduced by 170.24% with three white space channels under the tolerance waiting time 90 ms. When the tolerance waiting time is more than 50 ms there is no great difference between the two white space channels setup and three white space channels setup. As discussed in previous section, most of the major cities in the U.S. has restriction of white space channels. Thus, the network carriers is able estimate the quality of service they can offer according to the resource they own, such as the number of white space channels, the power supply, etc.

We involve the previous measurement work of channel state in multiple cities in DFW metroplex area to study the population density variation in white space network design [64]. We choose the The achieved channel capacity is mapping to the

population distribution as in [64]. The user distribution is set as our measurements in 11:00 AM with 30 ms tolerance waiting time. The results are shown in Fig. 5.7.

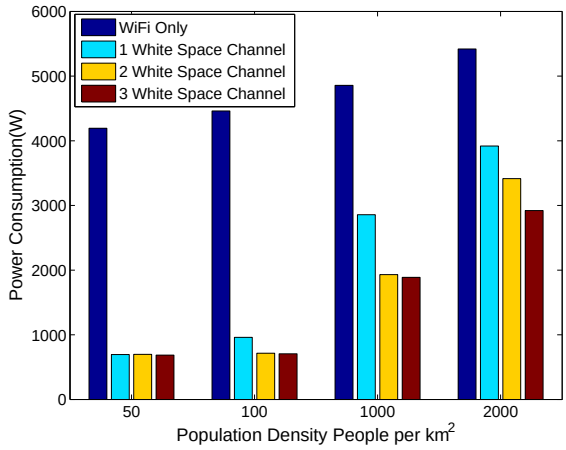

Figure 5.7: Power Consumption across Population Distribution

As the population increase, all the configuration of network cost more power to serve the users. The gains of a single white space channel reach the peak in 50 ppl/km^2 as 512.55%. And the users are able to be satisfied by only one white space channel, the increasing of white space channels does not gains in power consumption. The same result happens for 100 ppl/km^2 with more than two white space channels. The number of white space channels reaches the constant power consumption increase with the population. For 50 ppl/km^2 is one white space channel while 100 ppl/km^2 needs two white space channels. Also, the gain of a single white space channels decrease as the number of white space channels increase. Such as in 1000 ppl/km^2, the first white space channel gains 70% of power consumption, the second channel adding to the system gains only 47.98% and the third one gains only 2.26%. Thus, when the white space channels are limited, split them into multiple combination of WiFi cells could increase the power consumption other than put them in one WiFi virtual city.

We study the white space impacts on the WiFi mesh networks. The application of white space channels reduce the power consumption of the system most of the time. The white space channels are good at adapting user mobility with less power consumption. Through the numerical simulation, putting the limited white space channels as complementary resource for the existing wireless network is able to reduce the power consumption of the system or increase the quality of service. When the wireless resource is above a threshold, the gain of white space becomes relatively small in the system.

5.3. Conclusion

In this paper, we considered the use of few white space channel resource for improving the power consumption across a broad range of user mobility, population densities. To consider the power consumption of a system, we formulate the heterogeneous wireless network as a queuing system. We then analyze the heterogeneous queuing system based on previous queuing theory work. To address the resource allocation of white space channels, we proposed a Greedy Server-side Replace algorithm to find the resource allocation with minimum power consumption. We then perform spectrum utilization measurements in the typical areas of downtown, urban, campus, neighborhoods to drive the algorithm. We also leverage the user mobility pattern from WiEye measurements. Through extensive analysis across the spectrum utilization and user mobility, we show that white space bands can reduce the average of power consumption by 64.70% on average over 24 hours. We also integrated previous measurements work in north Texas and find the power consumption is reduced by white space bands by 512.55% in sparse area. In the future, we will consider to propose the heterogeneous wireless network deployment with large scale user mobility patterns.

Algorithm 5.1 Greedy Server-side Replace

Input:

N: Users

$H_{i,j}^{f}$: Vector of channel capacity

D: Traffic Rate

M: WiFi Cells

Find the WiFi cell with the lowest traffic rate D,break the tie with index
Calculate the power consumption according to Eq. 5.12 5.13 5.14
if If channel resource feasible and exist unserved traffic demand **then**
    List available options
    if Single channel is the best **then**
        Apply half-interval search to find the minimum capacity for the users
    else if Homogeneous is the best **then**
        Allocate the resource for the cell
        Keep the WiFi channel and find the minimum capacity for the users
    else if Heterogeneous is best **then**
        Adding white space resource to the cell
    end if
else
    Get the waiting time of the cell with all available resource
end if
Update the system information
Repeat the process for all the cells
Calculate the power consumption

Output:

The power consumption, resource allocation and the maximum waiting time

Chapter 6

Spectrum Adaptation for Multihop Access Networks

In this chapter, we illustrate the challenges of channel assignment in white space networks and formulate the problem of channel assignment when jointly using WiFi and white space bands. We present an ILP model to approach the optimal solution of the problem. Further, we present a measurement-driven algorithm to find the channel assignment with a reduced complexity.

6.1. Problem Formulation

In this section, we formulate the problem of how to optimally use WiFi and white space bands in concert when deploying wireless mesh networks. We first introduce the multiband mesh network system model and illustrate the challenges of such a WhiteMesh architecture in propagation and channel occupancy. We then discuss the network performance in economic view to evaluate WhiteMesh networks and the corresponding goal of both the optimization framework and the heuristic algorithm that we propose in the following section. Finally, we present our integer linear programming model used to address the problem.

6.1.1. WhiteMesh Network Architecture

A frequency band is commonly defined as a group of channels which have similar propagation characteristics with small frequency separation. A common assumption in previous works that use many WiFi channels is that the propagation characteristics of one channel is similar to another, since the channel separation is relatively small

(e.g., 5 MHz for the 2.4 GHz band). Many works which rely on such an assumption have focused on the allocation of multiple WiFi channels with multiple radios in multihop wireless networks with channels in one band [27]. However, as FCC licensed the white space bands for communication, the propagation variation has to be considered in wireless network.

Moreover, the FCC has flexible rules all over the states because of the existing TV stations and devices working in white space bands [7]. These existing channel occupancy has to be considered in the wireless communication with white space frequency [29]. To quantify the channel occupancy, we have the concept activity level in Eq. 2.2 and we apply the concept through Eq. 5.7.

Wireless mesh networks are a particular type of multihop wireless network that are typically considered to have at least two tiers [20]: *(i)* an access tier, where client traffic is aggregated to and from mesh nodes, and *(ii)* a multihop backhaul tier for connecting all mesh nodes to the Internet through gateway nodes. In this work, we focus on optimally allocating white space and WiFi bands on a finite set of radios per mesh node along the backhaul tier, since we assume that client devices will use WiFi (due to the economies of scale) along access tier. In each of the WhiteMesh topologies studied in Section 6.3, a sufficient number of orthogonal WiFi channels remain for the access tier clients connection through additional radios co-located on the mesh nodes.

In this work, we consider the diverse propagation characteristics for four frequency bands: 450 MHz, 800 MHz, 2.4 GHz, and 5.8 GHz. We refer to the two former frequency bands as white space (WS) bands, whereas the two latter frequency bands as WiFi bands. Due to the broadcast nature of the wireless medium, greater levels of propagation induce higher levels of interference. Also, the more allowed frequency channels and low level signal activity of white space bands co-exist in sparse areas.

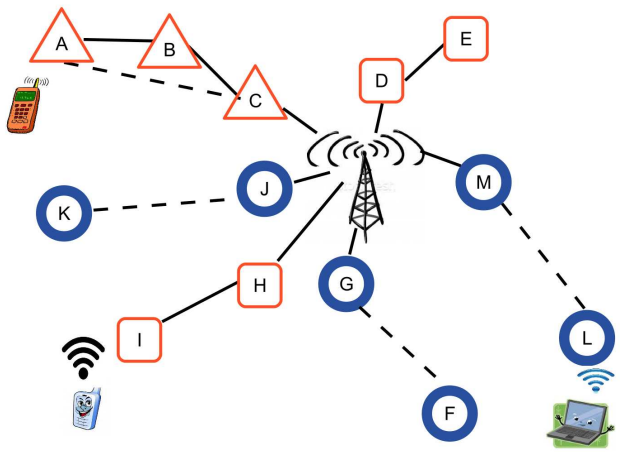

Figure 6.1: Example WhiteMesh topology with different mesh-node shapes representing different frequency band choices per link.

Thus, in sparsely-populated rural areas, the lower frequencies of the white space bands might be a more appropriate choice for multihop paths to gateways having reduced hop count with more capacity. However, as the population and demand scales up (e.g., for urban regions), the reduced spatial reuse and greater levels of interference of white space bands might detract from the overall channel assignment strategy. In such urban areas, select links of greater distance might be the most appropriate choice for white space bands, especially since the number of available channels is often inversely proportional to the population (due to the existence of greater TV channels).

Figure 6.1 depicts an example where mesh node A could connect to mesh node C through B at 2.4 GHz, or directly connect to C at 450 MHz. If 2.4 GHz were used, link D, E might be able to reuse 2.4 GHz if they are out of the interference range. However, if link A, C used 450 MHz, a lower hop count would result for the path, but lower levels of spatial reuse also result (e.g., for link D, E). While the issues of propagation, interference, and spatial reuse are simple to understand, the joint use of white space and WiFi bands to form optimal WhiteMesh topologies is challenging

since the optimization is based on the knowledge of prior channel assignment which is not available before the work has been finished.

6.1.2. Model and Problem Formulation

Multiband wireless network involve the propagation variation and channel occupancy additional to the previous multichannel scenario. Thus, we improve the prior multi-channel models [83, 27] to adopt the new parameters. In these previous models, they fail to distinguish the communication range D_c, interference range D_r and channel capacity variation across frequency bands. While these works would attempt to minimize the interference in a multihop network topology by an optimal channel assignment for a given set of radios, we hypothesize that using radios with a greater diversity in propagation could yield overall network performance gains. Therefore, for a given set of radios, we allow the channel choices to come from multiple frequency bands (i.e., multiband channel assignment, which also includes multiple channels in the same band). In this work, we assume all channels have the same bandwidth and adjust the channel capacity of each band through the measured channel occupancy parameter activity level 5.7. In practice, we could easily calculate the proportional ratio of channels in each band according to their bandwidth. We assume that the locations of mesh nodes and gateway nodes are given and all mesh nodes have radios with the same transmit power, channel bandwidth, and antenna gain. Each mesh node operates with a classic protocol model [37].

A mesh network could be represented by a unidirectional graph $G = (V, E)$, where V is the set of mesh nodes, and E is the set of all possible physical links in the network. If the received signal (according to Eq. 2.1) between two mesh nodes i, j for a given frequency band (from the set of all bands B) is greater than a communication-range threshold, then a data link exists and belongs to the set L with a fixed, non-zero capacity δ with a protocol model. Due to the frequency occupancy, the available channel

capacity could be calculated through Eq. 5.7 with new notation δ, δ_r represents C, C_r.

The capacity of a clean channel is denoted by δ. Under the protocol model, the capacity of a channel with interference of existing signals δ_r could be represented as the remaining free time of the channel capacity according to the measured activity level A. We employ the activity level based on multiple measurements in the target area to represent the average inter-network interference. Correspondingly, a connectivity graph C is formed for each band in B such that $C = (V, L, B)$. If the received signal for a given band is above an interference-range threshold, then contention occurs between nodes. We extend the conflict matrix in [83] related to different interference per band according to $F = (E_{i,j}, I_{Set}, B)$, where $E_{i,j}$ represents the link and I_{Set} includes all the links are physically inside the interference range D_r when operating on each band $b \in B$.

Therefore, the problem we model is: to choose the connectivity graph C' which maximizes the metrics obey the constraints of multiband wireless network (defined below). A key challenge is that selecting the optimal channels from the set B leads to a conflict graph F which cannot be known *a priory*. Previous works have proposed several coloring, cluster-independent set, mixed linear integer methodology for a single band b [63, 83, 27]. However, these works do not address a reduction in hop count or an increase in spatial reuse and channel occupancy for a set of diverse bands B.

In network application, the bottleneck of mesh network capacity has been shown to be the gateway's wireless connections [74]. The metric we use to evaluate the proposed algorithm is the traffic arrived at gateway nodes. Networks are operated and maintained by vendors, such as AT&T, T-Mobile, who charge the customers based on their data through Internet. Thus, we use random generated numbers to represent clients' traffic demands. The traffic arrived at gateway nodes correlated to the population of the area since people have almost traffic demand in long term average. The

employed performance metric of traffic arrived gateway X, is represented the traffic arrived at the gateway nodes, where in Eq. 6.1:

$$X = \sum_{w \in W, v \in V} T(w, v) \tag{6.1}$$

The traffic arrived gateway node $w \in W$ considers all incoming and outgoing wireless traffic from access node $v \in V$ as T onto the Internet. Obviously, the traffic arrived gateway is also related to the routing and other factors, we use a simple routing method to keep the maximum the traffic arrived at the gateway nodes, the exact calculation of gateway traffic arrived gateway is described in Section 6.3 and consider where to put the gateway nodes are outside the scope of this work.

6.1.3. Mixed Integer Linear Programming Formulation

To clarify the problem and approach the optimization solution of the problem, we present a mixed integer, linear programming formulation for optimizing channel assignment in multiband scenario. We assume that the set of available mesh nodes (V), gateways (W), and available bands (B) are pre-known. The communication links and conflict graph are given as parameters. The capacity δ_b is given as the available channel capacity according to activity level measurement noted in 5.7.

Sets:

V	set of nodes
B	set of bands

Parameters:

δ^b	$b \in B$	capacity of band b in target area
$I^b_{ij,lm}$	$(i,j,l,m) \in V, b \in B$	Protocol Interference of link (i,j) on band b brought by link (l,m)
W_i	$i \in V$ *binary*	Gateways in network
D_{di}	$i \in V$	Downlink demand of node i
D_{ui}	$i \in V$	Uplink demand of node i

In the variable set, we define a time share represents the percentage of time a single link transmits according to $\alpha^b_{i,j}$ for link i,j between node i and node j in band b. There are two terms $uy^b_{i,j,k}$ and $dy^b_{i,j,k}$ defined as uplink and downlink flows:

Variables:

$0 \leq \alpha^b_{ij} \leq 1$	$b \in B, (i,j) \in N$	Time share of link (i,j) on band b
$0 \leq uy^b_{i,j,k}$	$(i,j,k) \in V, b \in B$	Uplink flow of node k on link (i,j) at band b
$0 \leq dy^b_{i,j,k}$	$(i,j,k) \in N, b \in B$	Downlink flow of node k on link (i,j) at band b

Our objective is represented for maximizing the traffic arrived at gateway (X) described in Eq. 6.1.

Objective:

$$Max \sum_i \sum_j \sum_k \sum_b (uy^b_{i,j,k} + dy^b_{j,i,k}) \;\; When\ w_j = 1 \tag{6.2}$$

In the ILP, the connectivity, uplink, and downlink constraints are represented as:

Connectivity Constraints:

$$\alpha^b_{i,j} + \alpha^b_{j,i} + \sum_l \sum_m (\alpha^b_{l,m} \cdot I^b_{ij,lm}) \leq \delta^b, i \neq j \tag{6.3}$$

$$\sum_i uy^b_{i,j,k} + \sum_i dy^b_{i,j,k} \leq r^b_{j,k} \cdot \alpha^b_{j,k} \tag{6.4}$$

Uplink Constraints:

$$\sum_{k}\sum_{b} uy^{b}_{i,i,k} \leq D_{ui}\ when\ w_k = 0, i \neq k \tag{6.5}$$

$$uy^{b}_{i,j,k} = 0 w_k = 1 \tag{6.6}$$

$$\sum_{i}\sum_{b} uy^{b}_{i,j,k} = \sum_{m}\sum_{b} uy^{b}_{j,m,k}\ when\ w_k = 0, i \neq k \tag{6.7}$$

$$uy^{b}_{i,j,i} = 0 \tag{6.8}$$

Downlink Constraints:

$$\sum_{j}\sum_{b} dy^{b}_{i,j,i} \leq D_{di}\ when\ w_i = 0 \tag{6.9}$$

$$dy^{l}_{i,j,k} = 0\ when\ w_k = 1 \tag{6.10}$$

$$\sum_{j}\sum_{b} dy^{b}_{i,j,k} = \sum_{m}\sum_{b} dy^{b}_{j,m,k},\ when\ w_k = 0, i \neq k \tag{6.11}$$

$$dy^{b}_{i,i,j} = 0 \tag{6.12}$$

In the constraints, (6.3) represents the summation of the incoming and outgoing wireless time share and the interfering links' wireless time share, which should all be less than 1. Constraint (6.4) represents the incoming and outgoing wireless traffic, which should be less than the link capacity for link i, j. Uplink constraints (6.5) and (6.6) represent that the summation of any wireless flow i, j should be less than the demand of node k. Constraints (6.7) and (6.8) are used to restrict the sum of all incoming data flows for a given mesh node k to be equal to the sum of all outgoing flows. Downlink constraints (6.9) and (6.10) are similar to (6.5) and (6.6) but in the downlink direction. Similarly, constraints (6.11) and (6.12) are downlink versions of (6.7) and (6.8).

Similar linear programs model is to solve channel assignment wireless networks have been proved to be NP-hard [90]. Our model jointly considers channel assignment factors and provides the methodology to achieve the optimization solution. When the

particular configuration is given, we further choose the objectives, parameters, and relax constraints to find the approaching solution for the network.

6.2. Path Analysis with Diverse Propagation

In this section, we discuss the influence of diverse propagation characteristics of the wide range of carrier frequencies of white space and WiFi bands in wireless networks. We then introduce our measurement driven heuristic algorithm for channel assignment in WhiteMesh networks.

6.2.1. Path Interference Induced on the Network

In WhiteMesh networks, multihop paths can be intermixed with WiFi for more spacial reuse and white space bands with less hops. To deal with the trade-off, we consider analyze the band choices reduce the number of hops along a path and the aggregate level of interference that hop-by-hop path choices have on the network (i.e., Path Interference induced on the Network).

Mesh nodes closer to the gateway generally achieve greater levels of throughput at sufficiently high offered loads. To combat such starvation effects, we treat each flow with equal priority in the network when assigning channels. In the worst case, all nodes along a particular path have equal time shares for contending links (i.e., intra-path interference). We start the channel assignment assuming that h mesh nodes are demanding traffic from each hop of an h-hop path to the gateway. If each link along the path uses orthogonal channels, then each link could be active simultaneously, otherwise they will complete with each other. We note each node along the path had traffic demand T_d, obviously the bottleneck link along the path would be the one closest to the gateway, and then next. Thus, the total traffic along the path $h \cdot T_d$ must be less than the bottleneck link's capacity δ estimated from the measurements.

In such a scenario, the h-hop mesh node would achieve the minimum served demand, which we define as the network efficiency. In general, the active time per link for an h-hop mesh node can be represented by $1, \frac{h-1}{h}, \frac{h-2}{h} \cdots \frac{1}{h}$. The summation of all active times for each mesh node along the path is considered the intra-path network cost.

Considering only intra-path interference, using lower carrier frequencies allows a reduction in hop count and increase in the network efficiency of each mesh node along the h-hop path. However, a lower carrier frequency will induce greater interference to other paths to the gateway (i.e., inter-path interference). Fig. 6.1 depicts such an example where links in different bands are represented by circles for 450 MHz, rectangles for 2.4 GHz, and triangles for the nodes which can choose between the two. Nodes A and C could be connected through two 2.4-GHz links or a single 450-MHz link. With 2.4 GHz, the interfering distance will be less than using 450 MHz. For example, only link D, E will suffer from interference, whereas H, I would not. However, with 450 MHz, link A, C would interfere with links F, G, M, L, and K, J. At each time unit, the number of links interfering with the active links along a path would be the inter-path network cost.

When an h-hop flow is transmitted to a destination node, it prevents activity on a number of links in the same frequency via the protocol model. The active time on a single link can be noted as $\frac{T}{\gamma_h}$. An interfering link from the conflict matrix F counts as I_h per unit time and contributes to the network cost in terms of: $\frac{hT}{\gamma_1} \cdot I_1 + \frac{(h-1)T}{\gamma_2} \cdot I_2 \cdots \frac{T}{\gamma_h} \cdot I_h$. Then, the traffic transmitted in a unit of network cost for the h-hop node is:

$$E_\eta = \frac{T}{\sum_{i \in h} \frac{(h-i+1) \cdot T}{\gamma_i} \cdot I_i} \tag{6.13}$$

Using network efficiency, the equation simplifies to:

$$E_\eta = \frac{\gamma}{\sum_{i \in h} (h - i + 1) \cdot I_i} \tag{6.14}$$

The network efficiency is the amount of traffic that could be offered on a path per unit time. With multiple channels from the same band, I_i will not change due to the common communication range. With multiple bands, I_i depends on the band choice due to the communication range diversity. This network efficiency jointly considers hop count and interference. We define the Path Interference induced on the Network (PIN) as the denominator of Eq. 6.14, which represents the sum of all interfering links in the network by a given path. PIN is used to quantify the current state of channel for channel assignment across WiFi and white space bands. To determine when the lower carrier frequency will be better than two or more hops at a higher carrier frequency, we consider the average interference $\bar{I}$ of a given path at the higher frequency. The problem could be formulated as:

$$\frac{\gamma}{\frac{h(h-1)}{2} \cdot \bar{I} + I_x} \geq \frac{\gamma}{\frac{h(h+1)}{2} \cdot \bar{I}} \tag{6.15}$$

Here, from Eq. refeq:benefit when $I_x \leq 2 \cdot h\bar{I}$, the performance of a lower-frequency link is better than two higher-frequency hops for the same destination node. I_x is also a parameter of hop count in Eq. 6.14. When the hop count is lower which closer to the gateway node, the threshold would be more strict since the interference would have a greater effect on the performance.

6.2.2. Band-based Path Selection (BPS) Algorithm

We design a Band-based Path Selection (BPS) algorithm (described in Alg. 6.1) which first chooses the mesh node that has the largest physical distance from the gateway nodes to reduce the whole time cost of the network. When a path is constructed for the mesh node with the greatest distance, all subsequent mesh nodes along the path are also connected to the gateway. The intuition behind the BPS algorithm is to improve the worst mesh node performance in a path. In large-scale mesh networks, it is impractical to traverse all the paths with different combination of bands from

Algorithm 6.1 Band-based Path Selection (BPS)

Input:

M: Set of mesh nodes

G: Set of gateway nodes

C: Communication graph of potential links among all nodes

I: Interference matrix of all potential links

B: Available frequency bands

δ: Measurements based Channel Capacity

Output:

CA: Channel Assignment of the Network

1: Rank mesh nodes in Set M according to physical distance from gateway nodes G

2: Initialize $S_{curr} = G$, $N_{srv} = \emptyset$, $N_{unsrv} = M$,$I_{active} = \emptyset$

3: **while** $N_{srv} =! M$ **do**

4: Select node with largest distance to gateway

5: Find the adjacency matrix across band combinations A_c

6: **for all** $A_i \in A_c$ **do**

7: Find the shortest path SP_i in mixed adjacency matrix A

8: **for all** Link $l \in SP_i$, ordered from gateway to mesh node **do**

9: Find the least interfering path with measured $\delta \times E_n$

10: If equally-interfering links, choose higher frequency

11: Calculate the path interference of SP_i

12: **end for**

13: Store the shortest path SP_i as SP

14: **end for**

15: Assign the path in the network

16: Update N_{srv}, N_{unsrv}

17: Update I_{active} from I

18: **end while**

Output CA as the locally-optimal solution

a mesh node to any gateway node since it is a NP-hard problem. However, based on the discussion in Section 6.2.1, if two paths have the same number of used bands along those paths, then the path with the least hops is likely to have the greatest performance and is chosen. Similarly, if two path have the same path interference, we choose the path which has higher-frequency links for spatial reuse. Thus, the next step of the algorithm is to find the shortest path across band combinations.

To run the algorithm, compared to the number of mesh nodes, the amount of channels N_B in different bands is small. The time complexity of calculating the combination is $O(2^{N_B})$. Finding the shortest path in Dijkstra algorithm will cost $O(N_E^2)$ according to [35], where N_E is the set of possible links in the network, and as a result, the total complexity would be $O(N_E^2 \cdot 2^{N_B})$. The algorithm would then calculate the PIN of the candidate path and select the path with the least interference channel induced on the network for the source mesh node. After a path is assigned, the algorithm updates the network's channel assignment with served nodes, activated links, and radio information. Then, we iteratively assign channels for all the mesh nodes in the network.

If all the nodes are connected to gateway nodes ($N_E = \binom{n}{2}$ which is $O(N_V^2)$), then the complexity of assigning a channel for a mesh node is $O(N_E^2 \cdot 2^{N_B})$. Then, the complexity of assigning a mesh node is $O(N_V^4 \cdot 2^{N_B})$. To assign *all* the nodes in the network, the complexity would be $O(N_V^5 \cdot 2^{N_B})$. The complexity is polynomial time of the number of traffic demands points (client group) for a wireless network assignment.

6.3. Evaluation of WhiteMesh Channel Assignment

We now extensively evaluate our proposed measurement-driven heuristic algorithm against the upper bound approaching formed by our integer linear program and versus prior channel assignment strategies. We introduce the topologies and

metric calculation used in the analysis and present a set of results based on the linear program and heuristic algorithm.

6.3.1. Experimental Evaluation Setup

A key aspect of WhiteMesh networks is the diversity in propagation from the lowest white space channels (tens to hundreds of MHz) to the highest WiFi channels (multiple GHz). Thus, to evaluate the performance of our measurement-driven algorithm, we consider a wide range of propagation characteristics from four different frequency bands. For white space bands, we choose 450 and 800 MHz, for WiFi bands, we choose 2.4 and 5.8 GHz according to the measurements from [64]. In the 9 measurements from [64], we map the population density from US census [9] to the activity level for each bands as Table. 6.1. The measurements connect the relation of population distribution, traffic demand, and available channel capacity in multiple bands. We input the measurements to the ILP and heuristic algorithm to calculate the available channel capacity δ for our algorithm which makes the available channel capacity of all the bands more practical. With the same transmission power and antenna gain, the highest carrier frequency would have the shortest communication range. Hence, we set a communication-range threshold of -100 dBm, and normalize the communication range with the highest frequency of 5.8 GHz. In particular, the communication range of 450 MHz, 800 MHz, 2.4 GHz, and 5.8 GHz would be normalized to 12.8, 6.2, 2.4, and 1, respectively according to Eq. 2.1. The interference range is computed as twice that of the communication range [67]. We deploy static wireless mesh networks of n mesh nodes along a regular grid with a normalized distance of 0.8 between rectangular edges. The gateways are chosen through a typical cell hexagon deployment method based on 2.4 GHz [57]. Unless otherwise, specified in the analysis, all four bands are used in the WhiteMesh topology studied. For practical application scenarios, more channels could be involved in the algorithms.

The throughput achieved through the gateways is not only critical for network vendors (e.g., cellular carriers charge fees for total bandwidth through towers), but also has been used by researchers to evaluate channel assignment [14]. As mentioned previously, the wireless capacity of gateway nodes has been shown to be the bottleneck in mesh networks [73]. Moreover, traffic arrived gateway is affected by multiple factors, such as mesh node placement, gateway placement, routing, and channel assignment, the latter of which is the focus of our analysis and algorithms. For the purposes of our analysis, we specifically calculate the traffic arrived gateway first introduced in Section 6.1.2 in the following way. Mesh nodes that have a close hop count path to the gateway nodes are the first ones served. Where there are nodes with the same hop count, the least interfering mesh nodes are chosen for serving. Then, the demand of multihop mesh nodes are served until there is no remaining demand to be satisfied or there is no remaining channel capacity through any path.

Through the algorithms, we investigate the impacts of network size, bands availability, and channel occupancy on wireless white mesh networks. We vary the average population distribution and the available channel capacity according to [64] of the target area, assuming 10% of the residents will use our service. An individual would have a 100 KB/s traffic demand on average. Then, we assign the demand to users randomly under the same average value across the area and run the analysis of each case 20 times as the simulation configuration. Through the assignment, the traffic arrived at gateway nodes and the network throughput are calculated. To approach the traffic arrived gateway up-bound, we relax our ILP model to keep the link capacity constraints, given the demand of the mesh nodes as a parameter to achieve the maximum throughput at the gateways. We compare BPS with the *(i)* Common Channel Assignment (CCA) from [28], *(ii)* Breath First Search Channel Assignment (BFS-CA) from [83] under the same configuration. In typical CCA [28] algorithm,

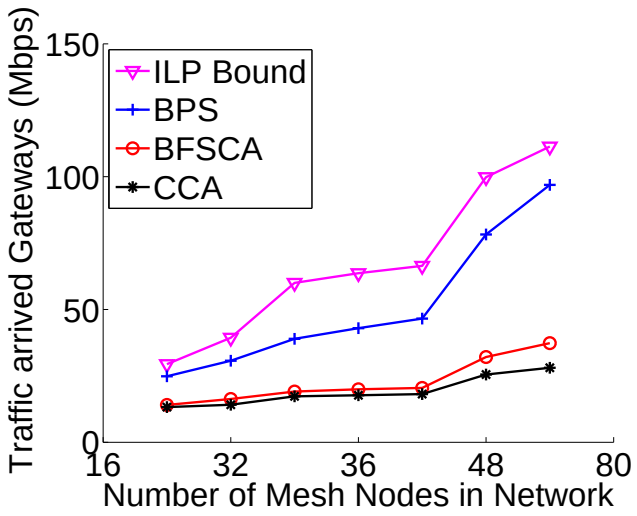

Figure 6.2: Average Population Distribution = 500 ppl/km^2

two nodes will assign a common channel for each other when both of them share free radios working in the same channel. In BFS-CA [83] algorithm, a node will search all the available one-hop connections then choose the one has the largest available capacity for a new assignment. These two methods focus on multi-channel assuming the existing links are equal when there is no assignment on the channel. In BPS, we both consider and leverage propagation differences of diverse bands. The ILP Bound calculation make the mesh nodes activate all possible connection the gateways if there exists a path. However, the three heuristic algorithms provide assignment each mesh node has connection only to one gateway in the network, and this reduce the dynamic changes for the assignment, which could be implemented by updating the assignment in a short term through the heuristic algorithms.

6.3.2. Experimental Analysis of WhiteMesh Backhaul

6.3.2.1. Network Size & Bands Effect

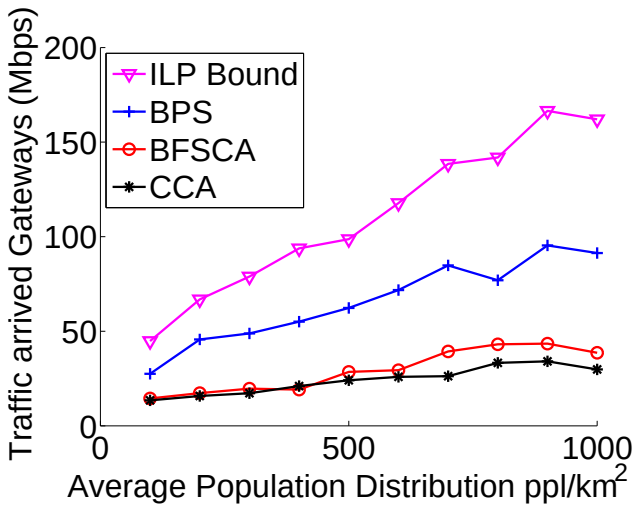

Figure 6.3: Varying Load, 49-Nodes Regular Grid

Typically, clients and mesh nodes have diverse traffic patterns with the download direction dominating the total traffic demand (e.g., consider service agreements for cellular data or Internet connectivity). Hence, to simplify the analysis and scale the ILP Bound to larger network sizes, we only consider the download traffic while maintaining the simulations. We then assign distributed download traffic demand randomly per mesh node with a maximum offered load to simulate the practical scenario as specified in Fig. 6.2, 6.3 and Table 6.2. We average the results of 20 simulations each of the algorithms for the given network configuration and compare the results to analyze multiband application in wireless network.

First, we investigate network sizes impacts on wireless white mesh network. The number of mesh nodes is varied from 16 to 64 in the aforementioned regular grid. As the network size grows, so too does the number of gateways through the hexagon gateway nodes deployment. Fig. 6.2 shows the total traffic arrived gateways when the population distribution is 500 ppl/km^2 for the ILP formulation and the heuristic algorithms: *(i)* Common Channel Assignment (CCA) from [28], *(ii)* Breadth First Search Channel Assignment (BFS-CA) from [66], *(iii)* our algorithm BPS (Section 6.2.2).

Frequency Bands	Population Distribution ppl/km^2								
	1500	1000	500	300	200	150	100	20	10
450 MHz	24.37	25.83	23.77	6.05	12.50	14.03	7.00	0.07	0.02
800 MHz	4.40	16.49	4.77	5.22	5.07	4.43	3.87	4.20	3.60
2.4 GHz	15.87	34.95	2.60	2.03	2.03	2.77	2.07	1.60	0.80
5.2 GHz	19.70	35.46	1.53	1.93	1.93	1.33	1.27	2.07	2.10

Table 6.1: Activity Level under Population Distribution

In Fig. 6.2, we observe as the network size increase, the performance gap among BPS and CCA/BFS-CA goes up. When the network size which represent the size of target area, the multiband wireless network has similar communication and interference performance with the multi-channel wireless network since all the nodes are located in a limited space where could be communicated/interfered by all the bands. As network size increase, the connection/interference variation among multiple bands makes the performance of multi-channel algorithms stay in low level. The ILP Bound shows what could be expected, that an increasing number of gateways/mesh nodes produce an increase in total traffic arrived gateways. However, we observe that CCA, BFS-CA algorithms are not able to achieve such behavior for various reasons. CCA fails to employ the communication range variation and find the most efficient hop connections which increase the average hop count. BFS-CA optimizes the first connection hop from the gateway, but fails to deal the whole path from the gateway to destination node. Conversely, BPS alleviates the strain on these first-hop, bottleneck links, achieving average 76% of the ILP Bound. The gap of BPS to the ILP is part from that the BPS only considers static one path to a gateway node for each mesh node, whereas the ILP allows multiple paths to the gateways. For BPS and other heuristic algorithms the dynamic assignment could be implemented through updating the assignment in a short term.

Next, we consider a different form of scalability in our analysis. Namely, we increase the average population distribution from 100 to 1,000 per km^2, while maintaining a 49-node regular grid topology. In the simulation set up, we map the channel capacity to the closest population measurement results. If there are measurements has the same distance to the current set up, the lower population measurement will be chosen, for instance, we map $400ppl/km^2$ to $300ppl/km^2$ measurements as shown in Table. 6.1. In Fig. 6.3, it shows that as the population distribution increases, the ILP and BPS diverge greatly from the remaining algorithms. Similar to Fig. 6.2, the wireless channel capacity around a gateway is quickly saturated if the algorithm is not focused on preserving that resource. Another factor of the performance is the channel capacity, as population increase the measured channel capacity vary in different bands. As the population reaches 1,000, the traffic arrived gateways decrease due to the channel capacity and the saturation of wireless channel capacity around the gateway nodes. BPS has an average performance of 60% of the ILP Bound, on average. CCA and BFS-CA fails to serve more traffic demand through the jointly WiFi and white space wireless network.

WhiteMesh networks could be deployed across a vast array of environments, from rural to urban areas. Each of these areas will have varying amounts of user demand traffic in proportion to the population densities. However, since a greater number of TV stations exist in urban areas, the available white space bands are often inversely related to the population density due to the FCC rules [5]. Also the available channel capacity is related to the existing signal activities in the area. To capture these varying degrees of demand and white space availability we consider three likely scenarios and one final scenario for comparison purposes: *(i)* two WiFi bands (2.4 and 5.8 GHz) channels with two white space channels (450 and 800 MHz), *(ii)* three channels in two WiFi bands (2.4 and 5.8 GHz) with one white space channel (450 MHz), *(iii)* Four

Bands/ Algorithms	WiFi Only	WS Only	WS & WiFi	WS & WiFi	WS & WiFi	WS & WiFi
WS (MHz)		450,800	450	800	450	800
WiFi (GHz)	2.4, 5		2.4	2.4	5	5
CCA [28]	22.4	13.4	13.2	12.5	16.9	23.2
BFS-CA [66]	26.3	15.8	14.9	19.4	22.7	28.4
BPS (Alg. 1)	41.2	34.1	38.2	40.0	35.4	42.8

Bands/	WS &	WS &	Multi-WS &	Multi-WS &	Multi-WS &
Algorithms	Multi-WiFi	Multi-WiFi	WiFi	WiFi	Multi-WiFi
WS (MHz)	450	800	450,800	450,800	450,800
WiFi (GHz)	2.4, 5	2.4, 5	2.4	5	2.4, 5
CCA [28]	24.1	30.6	25.2	23.9	30.4
BFS-CA [66]	38.9	33.7	30.1	27.4	36.6
BPS (Alg. 1)	58.4	64.9	54.4	51.9	63.1

Table 6.2: Throughput achieved through Gateway nodes (Mbps) for various combinations of WiFi and Average Population Distribution = 500 ppl/km^2, Network Size = 49 mesh nodes).

channels in two WiFi bands (2.4 and 5.8 GHz) without any white space channels, and *(iv)* four channels in two white space bands (450 and 800 MHz) with no WiFi bands (for comparison).

Table 6.2 describes the achieved traffic arrived gateways for various combinations of WiFi and white space bands with a maximum offered load of 5 Mbps from 500 ppl/km^2 in a regular 49-node grid. We consider the performance of BPS in the four aforementioned scenarios of varying white space availability. A regular, 49-nodes grid is again used. In the simulation, we keep 4 channels for each method, such as in the combination of 2.4 GHz and 5 GHz, we put 2 channels in both bands. In the triple bands combinations, we set each band has a channel, and put the other channel

in the highest frequency band. (In 2.4 GHz, 5GHz, 800 MHz combination, we put the extra channel other than the 3 channel each band in 5 GHz). Immediately, we observe that the WiFi-only scenario has greater traffic arrived gateways than the white-space-only scenario. This is due to the lack of spatial reuse achieved by white spaces. White space has larger communication to shorten the hop counts as well as has larger interference reducing the spatial reuse. Another reason is that the available channel capacity of 500 ppl/km^2 in white space bands are worse than WiFi bands. This two reasons make the white space only has worse performance no matter what channel assignment methods are applied. Interestingly, however, the joint use of both white space and WiFi bands has significant gains over the single type of band scenarios with the same number of channels (40% greater than WiFi and 56% over white space, on average).

In 500 ppl/km^2 scenario, 5 GHz channel is cleaner than 450 MHz which makes the combination of 2 channels in 5 GHz, 1 channel in 2.4 GHz and 800 MHz has better performance than WiFi(2)+WS(2) in some cases. Obviously, in Table 6.2 that with the same number of available bands (2), when the combination has similar propagation characters, such as one in WiFi band, one in white space band, the combination has clean channels have better performance. With similar channel capacity, lower frequency offers more option for connection path could output a better channel assignment. If we have one channel in a white space band and one channel in a WiFi band, then we could use the advantage of both WiFi for spatial reuse and white spaces to reduce the hop count.

6.3.2.2. Effect of Channel Occupancy

In Fig. 6.4, we show the impacts of channel occupancy through the activity level and spacing variation on wireless white space mesh network. The activity level defined in 2.2 represent the available channel capacity. The spacing gap is related to the

population distribution according to the hexagon deployment for access tier network deployment, the more population distribution, the smaller spacing gap between mesh nodes. In the simulation, we assume all the bands have the same activity level and use the 49-nodes regular grid with normalized multiple spacing distance gap from 0.2 to 2.1. From the 3-D figure, we could see as the activity level increase, the traffic arrived gateways decrease due to the deduction of available channel capacity. In the spacing dimension, when the nodes have small spacing gap, all the bands could not be applied for spatial reuse, the traffic arrived gateways is small. But as the spacing gap increase, the spatial reusing is available for high frequency bands, the traffic arrived gateways increase. Then, as the spacing gap increase over the high frequency communication range, the number of usable channels start to decrease according to protocol model, the traffic arrived gateways decrease in the figure.

We further investigate the spacing gap variation under in-field scenario. The in-field measurement mapping is listed in Table. 6.1. We keep the white mesh network as 49-nodes regular grid, assume each mesh node has 4 radios in each band. As clarified, a larger spacing gap between mesh nodes means less population. We map the largest population distribution in Table 6.1 to represent the spacing as normalized distance 0.2, and the least population distribution as normalized distance 1.7. In a regular grid the spacing distance D_s, population distribution P_d and mesh node capacity M_c should obey $P_d \cdot \frac{D_s}{2}^2 \propto M_c$. The 9 measured data sets are mapped to generate the matrix sets. Then according the data in the matrix we interpolate activity level for each normalized distance from 0.2 to 1.7 with gap 0.1. These data sets are put into the heuristic algorithms and the results are shown in Fig. 6.5.

In Fig. 6.5, as the space gap increase, the multiband network has better performance through spatial reuse matching the simulation analysis shown in Fig. 6.4. As the distance increase up to normalized distance 1, one of the channel in 5 GHz

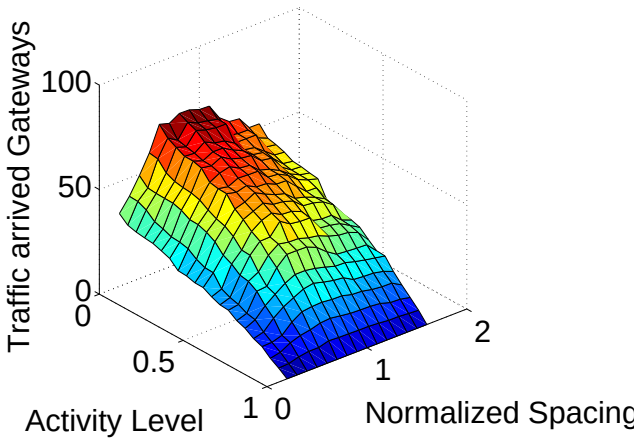

Figure 6.4: Uniform Activity Level VS. Space Distance

could not be applied in the network since the distance is larger than its communication range under the protocol model, that makes the performance decrease quickly. Through this investigation, we can conclude that in sparse area when the number of mesh nodes is small, lower frequency for the back-hual network could have better performance. However, in dense area when the mesh nodes are deployed closely, have higher frequency for spatial reuse is better than the low frequency white space bands.

Through these analysis, a mixed WiFi and white space wireless network could improve the performance in the scenarios as follow: *(i)* Larger network has more mesh nodes, which need more capacity from spatial reuse and flexible path to reduce hop count through more links. *(ii)* Rural area whose spacing gap among mesh nodes is larger. Not only for the number of mesh nodes reducing but also for hop count reducing. However, as we discussed, the flexible paths and the interference among these links become more critical at different points in the WhiteMesh topology. For the sake of completeness, we need cautious selection of frequency bands in wireless network deployment.

6.4. Summary

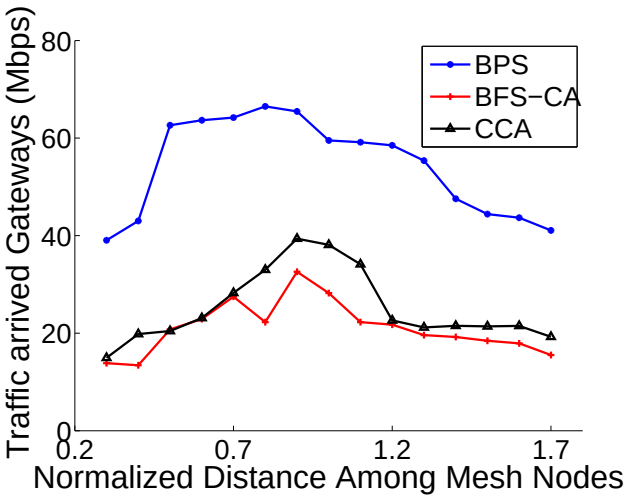

Figure 6.5: Traffic arrived Gateways with Activity Level & Spacing

In this chapter, we exploited the joint use of WiFi and white space bands for improving the served user demand of wireless mesh networks in practical scenarios. To do so, we used an integer programming model with in-field measurements to find optimal WhiteMesh channel assignment. We then constructed a measurement driven heuristic algorithm, Band-based Path Selection, to approach optimal performance with reduced complexity. Through extensive analysis across varying offered loads, network sizes, and white space channel availability, we show that our algorithm can achieve 180% the served user demand versus previous multi-channel, multi-radio solutions in multiband scenarios, since we leverage diverse propagation characteristics offered by WiFi and white space bands. Moreover, we quantify the degree to which the joint use of these bands can improve the served user demand. Our BPS algorithm shows that WhiteMesh topologies can achieve up to 160% of the traffic arrvied gateways of similar WiFi- or white-space-only configurations.

Chapter 7

Related Work

As FCC adopt the white space bands for communication, the application of these new frequency resource become new research spot. Many previous works are related to the challenges for white space frequencies, but no one focused on and answered on them.

7.1. White Space Links

A bunch of work has been done on radio-scene analysis and channel identification for utility of channel adaptation dating back to Simon Haykin [39]. Some work of Multi-bands/Multi-channels in cognitive radios focus on optimize performance, such as avoiding frequency diversity [65]. In [77] an opportunistic algorithm is introduced to balance the cost of spectrum sensing and channel switching in multichannel scenario.

Oppose to previous works, our work is motivated by prospective releasing frequency, white space bands used for TV and exploit the comparison across all the available bands in the future. Previous work assume all the channels have the same performance in an clean environment for channels with small gap of frequencies. However, when the white space bands are activated, the assumption need to be adjust due to the propagation variation of the channels with large gap in frequency. Some other works focus on the theoretic stopping rules of spectrum sensing with the cost of time and channel switching gains [76, 77]. In contrast, we focus on measurement driven framework to exploit the channel selection rules under in-field environment and to

leverage the impacts of white space bands on wireless communication links.

7.2. White Space Networks

Prior work in wireless network deployment has focused extensively on solving gateway placement, channel assignment, and routing problems to reduce the interference generated inside the network [40, 66, 11]. Unfortunately, few works in network deployment notice the interference across networks. Some cognitive radio works discuss this inter-network interference, but most of them focus on point-to-point communication other than taking a network-wide view [19].

With new FCC regulations on the use of white space bands, there are two factors to consider with such bands: large propagation range and existing inter-network interference from TV stations and other devices such as microphones [5, 25, 15]. Prior work does not specifically study the benefits of jointly using white space and WiFi bands in the deployment of wireless access networks [12]. Additionally, prior work related to white spaces target opportunistic media access. However, the application of white spaces across diverse population densities has not been fully explored.

Finally, some works discuss the propagation variation in both WiFi bands and white space bands. For example, Robinson et al. models the propagation variation at the same band in terrain domain [73]. Another work proposes a database-driven framework for designing a white space network with database of primary user (TV station) locations and channel occupation [60]. However, these works do not jointly study the influence of white space and WiFi bands on network deployment according to their resulting propagation variation and spectrum utilization.

Wireless mesh network deployment is to design wireless architecture for offering Internet service in an target area. There are significant challenges in wireless mesh network deployment, such as user priorities, user behaviors, long term throughput es-

timation, selfish clients, interference and energy efficiency, etc. [84] These challenges are distinguished under the topics of channel assignment, cognitive radio, protocol design, etc. [84, 11] Previous works have recognize the impact of interference in wireless mesh network deployment is the key issue [83, 43, 23]. To overcome the challenges, a lot of works have been done to optimize the deployment in increasing throughput, minimize resource, reducing interference, etc. [43, 81, 27] Many works have studied the network deployment problem in multihop wireless networks [45, 12, 68, 84]. In addition, multiple radios have been used to improve the routing in multi-channel scenarios [28, 43]. Both static and dynamic network deployments have been discussed in previous works under the 802.11 WiFi scenario [88, 66, 81]. However, all of the aforementioned works have not considered propagation differences of the diverse frequency bands of white space and WiFi, which we show are critical improving the performance of mesh networks. Frequency agility in multiband scenario brings more traffic capacity to wireless network deployment as well as more complexity of resolving the interference issues.

Previous work [64] involve the inter-network interference in multiband scenario, but did not offer the solution of intra-network interference. As a new designed wireless network, intra-network interference is more important for performance estimation. Previous work focus on WiFi wireless networks proposed several methods to reduce the interference targeting on multiple metrics. [83, 40, 73] focus on reducing the gateway mesh nodes. [43, 81] try to reduce the overall interference in the worst case of traffic independent scenario. [23, 51] improve the performance in throughput. However, these works fails to involve the traffic demands of clients in their solutions. [73, 54] consider the QoS requirements in the WiFi network design. Our work also consider the traffic demands from the client as part of our network design to satisfy both customers and vendors.

The wireless network deployment problem has been proved as a NP-hard problem [27]. Several works introduce relaxed linear program formulation to find the optimization of multihop wireless networks [83, 43, 30]. Also, game theory methods is another option to solve the problem [67, 86]. Social network analysis is also popular in wireless network design [92]. In this work, we model the problem to a linear program to approach the optimal solution and generate heuristic algorithms to find a practical solution for the problem.

To be used effectively, white space bands must ensure that available TV bands exist but no interference exists between microphones and other devices [15]. White space bands availability has to be known in prior of network deployment. TV channels freed by FCC are fairly static in their channel assignment, databases have been used to account for white space channel availability (e.g., Microsoft's White Space Database [8]). In fact, Google has even visualized the licensed white space channels in US cities with an API for research and commercial use [7]. In contrast, we study the performance of mesh networks with a varying number of available white space channels at varying population densities, assuming such white space databases and mechanisms are in place. As FCC release these bands for research, many methods have been proposed to employ these frequency bands. [15] introduce WiFi like white space link implementation on USRP and link protocols. [25] discuss the point to point communication in multiband scenario. In [30], white space band application is discussed in cognitive radio network for reducing maintenance cost. In [26], the white space is proposed to increase the data rates through spectrum allocation. In our work, we focus on maximizing the throughput of the wireless network.

Since white space bands were free for wireless communication, many efforts have been put in the area for the application of white space bands. [5] In [15]. the author considered a cognitive method to avoid collision between white space communication

and TV broadcasting. Many works increasing the convenience of using white space databases have been published (e.g., Microsoft's White Space Database [8]). Google has even visualized the licensed white space channels in US cities with an API for research and commercial use [7]. Previous work discussed the point to point communication with white space bands [25], and the wireless network deployment with plenty white space channels [64]. However, many of the major cities in the US do not have plenty white space channels, such as most area of Austin, TX has only one white space channel. As far as we know, there is no work discuss these scenarios.

Applying white space in wireless network is similar to the previous multi-channel works other the propagation variation. In [18] a multi-channel system is formulated as a queuing system and Server Side Greedy algorithm is proposed to optimize the throughput with low complexity. In [46], Delay-based Queue-Side-Greedy algorithm is proposed with low complexity for optimal throughput and near-optimal delay. [52] develop a multi-objective optimization framework to minimal energy consumption in a multi-channel multi-radio system. However, these works do not address minimizing the resource for certain quality of service and assume an on-off channel model.

Previous work studied the multi user setting with a single channel [82]. Spectral diversity is isolated for a single user in [79]. In [53], multi-user dynamic channel access is proposed jointly consider the temporal and spectral diversity in a multichannel model. However, none of these works address the channel association problem in multiband scenario. Previous work [64] studied the white space application in access network deployment with spectral diversity. However, these works fails to leverage the white space frequency in multi-user diversity in both spectral and temporal scenarios.

Previous works in real time systems put many efforts to minimize the resources, such as processors [61]. In [50], the author proves the capacity augmentation bounds for schedulers of parallel tasks. However, these works assume the parallel tasks have

uniform servers. Previous work [21] investigate the white space in a queuing system without considering the heterogeneous topology. In contrast, we study the performance of a heterogeneous network with both white space channels and WiFi channels in channel utilization.

Chapter 8

Conclusion

REFERENCES

[1] Metis: Mobile and wireless communications enablers for the twenty-twenty information society.

[2] Cambria gw2358-4 network platform. http://www.gateworks.com/, 2007.

[3] Aximuth ACE-MIMO Channel Emulator. http://www.azimuthsystems.com, Mar. 2011.

[4] Openwrt wireless freedom. https://openwrt.org/, Dec. 2011.

[5] Fcc white space. `http://www.fcc.gov/topic/white-space`, 2012.

[6] Ubiquiti xtremerange series of radio. http://www.ubnt.com/, 2012.

[7] Google spectrum database. `http://goo.gl/NnIFXQ`, 2013.

[8] Microsoft research white space database. `http://whitespaces.cloudapp.net/Default.aspx`, 2013.

[9] People and households. `http://www.census.gov/people/`, 2014.

[10] Afanasyev, M., Chen, T., Voelker, G., and Snoeren, A. Analysis of a mixed-use urban WiFi network: When metropolitan becomes neapolitan. In *ACM IMC* (2008).

[11] Akyildiz, I. F., Lee, W.-Y., Vuran, M. C., and Mohanty, S. Next generation/dynamic spectrum access/cognitive radio wireless networks: a survey. *Computer Networks 50*, 13 (2006), 2127–2159.

[12] Akyildiz, I. F., Wang, X., and Wang, W. Wireless mesh networks: a survey. *Computer networks 47*, 4 (2005), 445–487.

[13] Andersen, J. B., Rappaport, T. S., and Yoshida, S. Propagation measurements and models for wireless communications channels. *IEEE Communications Magazine 33*, 1 (1995), 42–49.

[14] Avallone, S., and Akyildiz, I. F. A channel assignment algorithm for multi-radio wireless mesh networks. *Computer Communications 31*, 7 (2008), 1343–1353.

[15] Bahl, P., Chandra, R., Moscibroda, T., Murty, R., and Welsh, M. White space networking with WiFi like connectivity. *ACM SIGCOMM 39*, 4 (2009), 27–38.

[16] Balanis, C. A. *Antenna theory: analysis and design*. John Wiley & Sons, 2012.

[17] Banfield, R., Hall, L., Bowyer, K., Kegelmeyer, W., et al. A comparison of decision tree ensemble creation techniques. *IEEE Trans on Pattern Analysis and Machine Intelligence 29*, 1 (2007), 173.

[18] Bodas, S., Shakkottai, S., Ying, L., and Srikant, R. Low-complexity scheduling algorithms for multichannel downlink wireless networks. *Networking, IEEE/ACM Transactions on 20*, 5 (2012), 1608–1621.

[19] Cabric, D., Mishra, S., and Brodersen, R. Implementation issues in spectrum sensing for cognitive radios. In *Signals, Systems and Computers, 2004. Conference Record of the Thirty-Eighth Asilomar Conference on* (2004), vol. 1, Ieee, pp. 772–776.

[20] Camp, J., Robinson, J., Steger, C., and Knightly, E. Measurement driven deployment of a two-tier urban mesh access network. In *ACM MobiSys* (2006).

[21] Chen, S., Wyglinski, A. M., Pagadarai, S., Vuyyuru, R., and Altintas, O. Feasibility analysis of vehicular dynamic spectrum access via queueing theory model. *Communications Magazine, IEEE 49*, 11 (2011), 156–163.

[22] Cheng, J. Philadelphia's municipal WiFi network to go dark. `http://arstechnica.com/gadgets/2008/05/philadelphias-municipal-wifi-network-to-go-dark`, 2008.

[23] Chieochan, S., and Hossain, E. Channel assignment for throughput optimization in multichannel multiradio wireless mesh networks using network coding. *Mobile Computing, IEEE Transactions on 12*, 1 (2013), 118–135.

[24] Cui, P., Liu, H., He, J., Altintas, O., Vuyyuru, R., Rajan, D., and Camp, J. Leveraging diverse propagation and context for multi-modal vehicular applications.

[25] Cui, P., Liu, H., He, J., Altintas, O., Vuyyuru, R., Rajan, D., and Camp, J. Leveraging diverse propagation and context for multi-modal vehicular applications. In *IEEE WiVeC* (2013).

[26] Deb, S., Srinivasan, V., and Maheshwari, R. Dynamic spectrum access in dtv whitespaces: design rules, architecture and algorithms. In *Proceedings of the 15th annual international conference on Mobile computing and networking* (2009), ACM, pp. 1–12.

[27] Doraghinejad, M., Nezamabadi-Pour, H., and Mahani, A. Channel assignment in multi-radio wireless mesh networks using an improved gravitational search algorithm. *Journal of Network and Computer Applications 38* (2014), 163–171.

[28] Draves, R., Padhye, J., and Zill, B. Routing in multi-radio, multi-hop wireless mesh networks. In *ACM MobiCom* (2004).

[29] Fallah, Y. P., Huang, C., Sengupta, R., and Krishnan, H. Congestion control based on channel occupancy in vehicular broadcast networks. In *Vehicular Technology Conference Fall (VTC 2010-Fall), 2010 IEEE 72nd* (2010), IEEE, pp. 1–5.

[30] Filippini, I., Ekici, E., and Cesana, M. A new outlook on routing in cognitive radio networks: minimum-maintenance-cost routing. *IEEE/ACM Transactions on Networking (TON) 21*, 5 (2013), 1484–1498.

[31] Franklin, A. A., and Murthy, C. S. R. Node placement algorithm for deployment of two-tier wireless mesh networks. In *Global Telecommunications Conference, 2007. GLOBECOM'07. IEEE* (2007), IEEE, pp. 4823–4827.

[32] Friis, H. T. A note on a simple transmission formula. 254–256.

[33] Gelenbe, E., Pujolle, G., and Nelson, J. *Introduction to queueing networks*. Citeseer, 1998.

[34] Ghasemi, A., and Sousa, E. Spectrum sensing in cognitive radio networks: requirements, challenges and design trade-offs. *Communications Magazine, IEEE 46*, 4 (2008), 32–39.

[35] Golden, B. Shortest-path algorithms: A comparison. *Operations Research* (1976), 1164–1168.

[36] Google. Spectrum database. `http://www.google.org/spectrum/whitespace/`, 2013.

[37] Gupta, P., and Kumar, P. R. The capacity of wireless networks. *IEEE Trans. on Information Theory 46*, 2 (2000), 388–404.

[38] Hall, M., Frank, E., Holmes, G., Pfahringer, B., Reutemann, P., and Witten, I. The weka data mining software: an update. *ACM SIGKDD Explorations Newsletter 11*, 1 (2009), 10–18.

[39] Haykin, S. Cognitive radio: brain-empowered wireless communications. *Selected Areas in Communications, IEEE Journal on 23*, 2 (2005), 201–220.

[40] He, B., Xie, B., and Agrawal, D. P. Optimizing deployment of internet gateway in wireless mesh networks. *Computer Communications 31*, 7 (2008), 1259–1275.

[41] Hossain, E., Chow, G., Leung, V., McLeod, R., Mišić, J., Wong, V., and Yang, O. Vehicular telematics over heterogeneous wireless networks: A survey. *Computer Communications 33*, 7 (2010), 775–793.

[42] Inc., C. Fcc certifies carlson wireless technologies tv white space radio. `http://www.carlsonwireless.com/rural-connect-press-release.html`, 2014.

[43] Irwin, R. E., MacKenzie, A. B., and DaSilva, L. A. Resource-minimized channel assignment for multi-transceiver cognitive radio networks. *Selected Areas in Communications, IEEE Journal on 31*, 3 (2013), 442–450.

[44] Jacobson, V., Leres, C., and McCanne, S. The tcpdump manual page. *Lawrence Berkeley Laboratory, Berkeley, CA* (1989).

[45] Jain, K., Padhye, J., Padmanabhan, V. N., and Qiu, L. Impact of interference on multi-hop wireless network performance. *Wireless networks 11*, 4 (2005), 471–487.

[46] Ji, B., Gupta, G. R., Lin, X., and Shroff, N. B. Performance of low-complexity greedy scheduling policies in multi-channel wireless networks: Optimal throughput and near-optimal delay. In *INFOCOM, 2013 Proceedings IEEE* (2013), IEEE, pp. 2589–2597.

[47] Kanodia, V., Sabharwal, A., and Knightly, E. MOAR: A multi-channel opportunistic auto-rate media access protocol for ad hoc networks. In *Broadnets* (San Jose, CA, October 2004).

[48] Karrer, R., Sabharwal, A., and Knightly, E. Enabling large-scale wireless broadband: the case for TAPs. In *HotNets-II* (2003).

[49] Kim, S., Bertoni, H., and Stern, M. Pulse propagation characteristics at 2.4 ghz inside buildings. *Vehicular Technology, IEEE Transactions on 45*, 3 (1996), 579–592.

[50] Li, J., Chen, J. J., Agrawal, K., Lu, C., Gill, C., and Saifullah, A. Analysis of federated and global scheduling for parallel real-time tasks. In *Real-Time Systems (ECRTS), 2014 26th Euromicro Conference on* (2014), IEEE, pp. 85–96.

[51] Li, X., Wu, J., Lin, S., and Du, X. Channel switching control policy for wireless mesh networks. *Journal of Parallel and Distributed Computing 72*, 10 (2012), 1295–1305.

[52] Liu, L., Cao, X., Cheng, Y., Du, L., Song, W., and Wang, Y. Energy-efficient capacity optimization in wireless networks. In *INFOCOM, 2014 Proceedings IEEE* (2014), IEEE, pp. 1384–1392.

[53] Liu, Y., and Liu, M. To stay or to switch: Multiuser dynamic channel access. In *INFOCOM, 2013 Proceedings IEEE* (2013), IEEE, pp. 1249–1257.

[54] Long, Y., Li, H., Pan, M., Fang, Y., and Wong, T. F. A fair qos-aware resource-allocation scheme for multiradio multichannel networks. *Vehicular Technology, IEEE Transactions on 62*, 7 (2013), 3349–3358.

[55] Marina, M. K., Das, S. R., and Subramanian, A. P. A topology control approach for utilizing multiple channels in multi-radio wireless mesh networks. *Computer Networks 54*, 2 (2010), 241–256.

[56] Martello, S., and Vigo, D. Exact solution of the two-dimensional finite bin packing problem. *Management science 44*, 3 (1998), 388–399.

[57] Meguerdichian, S., Koushanfar, F., Qu, G., and Potkonjak, M. Exposure in wireless ad-hoc sensor networks. In *Proceedings of the 7th annual international conference on Mobile computing and networking* (2001), ACM, pp. 139–150.

[58] Meikle, R., and Camp, J. A global measurement study of context-based propagation and user mobility. In *Proceedings of the 4th ACM international workshop on Hot topics in planet-scale measurement* (2012), ACM, pp. 21–26.

[59] Mo, J., So, H., and Walrand, J. Comparison of multi-channel mac protocols. In *Proceedings of the 8th ACM international symposium on Modeling, analysis and simulation of wireless and mobile systems* (2005), ACM, pp. 209–218.

[60] Murty, R., Chandra, R., Moscibroda, T., and Bahl, P. Senseless: A database-driven white spaces network. *Mobile Computing, IEEE Transactions on 11*, 2 (2012), 189–203.

[61] Nelissen, G., Berten, V., Goossens, J., and Milojevic, D. Techniques optimizing the number of processors to schedule multi-threaded tasks. In *Real-Time Systems (ECRTS), 2012 24th Euromicro Conference on* (2012), IEEE, pp. 321–330.

[62] Niida, S., Uemura, S., and Nakamura, H. User tolerance for waiting time. *IEEE Vehicular Technology Magazine 5*, 3 (2010), 61–67.

[63] Peng, Y., Yu, Y., Guo, L., Jiang, D., and Gai, Q. An efficient joint channel assignment and QoS routing protocol for ieee 802.11 multi-radio multi-channel wireless mesh networks. *Journal of Network and Computer Applications* (2012).

[64] Pengfei Cui, Hui Liu, D. R., and Camp, J. A measurement study of white spaces across diverse population densities. *IEEE 10th WiNMeE* (2014).

[65] Rahul, H., Edalat, F., Katabi, D., and Sodini, C. Frequency-aware rate adaptation and mac protocols. In *Proceedings of the 15th annual international conference on Mobile computing and networking* (2009), ACM, pp. 193–204.

[66] Ramachandran, K. N., Belding-Royer, E. M., Almeroth, K. C., and Buddhikot, M. M. Interference-aware channel assignment in multi-radio wireless mesh networks. In *IEEE INFOCOM* (2006).

[67] Raniwala, A., and Chiueh, T. Architecture and algorithms for an IEEE 802.11-based multi-channel wireless mesh network. In *IEEE INFOCOM* (2005).

[68] Raniwala, A., Gopalan, K., and Chiueh, T.-c. Centralized channel assignment and routing algorithms for multi-channel wireless mesh networks. *ACM SIGMOBILE MCCR 8*, 2 (2004), 50–65.

[69] Rappaport, T. *Wireless Communications, Principles & Practice*. Prentice Hall, 1996.

[70] Rayanchu, S., Shrivastava, V., Banerjee, S., and Chandra, R. Fluid: improving throughputs in enterprise wireless lans through flexible channelization. In *Proceedings of the 17th annual international conference on Mobile computing and networking* (2011), ACM, pp. 1–12.

[71] Raychaudhuri, D., and Jing, X. A spectrum etiquette protocol for efficient coordination of radio devices in unlicensed bands. In *Personal, Indoor and Mobile Radio Communications, 2003. PIMRC 2003. 14th IEEE Proceedings on* (2003), vol. 1, IEEE, pp. 172–176.

[72] Reardon, M. EarthLink pays 5 million to delay houston Wi-Fi buildout. `http://news.cnet.com/8301-10784\_3-9768759-7.html`, 2007.

[73] Robinson, J., Singh, M., Swaminathan, R., and Knightly, E. Deploying mesh nodes under non-uniform propagation. In *IEEE INFOCOM* (2010).

[74] Robinson, J., Uysal, M., Swaminathan, R., and Knightly, E. Adding capacity points to a wireless mesh network using local search. In *IEEE INFOCOM* (2008).

[75] Rosston, G., Savage, S., and Waldman, D. Household demand for broadband internet service. *Communications of the ACM 54*, 2 (2011), 29–31.

[76] Sabharwal, A., Khoshnevis, A., and Knightly, E. Opportunistic spectral usage: Bounds and a multi-band csma/ca protocol. *Networking, IEEE/ACM Transactions on 15*, 3 (2007), 533–545.

[77] Sadeghi, B., Kanodia, V., Sabharwal, A., and Knightly, E. Opportunistic media access for multirate ad hoc networks. In *ACM MobiCom* (Sept. 2002).

[78] Shellhammer, S., Sadek, A., and Zhang, W. Technical challenges for cognitive radio in the tv white space spectrum. In *Information Theory and Applications Workshop, 2009* (2009), IEEE, pp. 323–333.

[79] Shu, T., and Krunz, M. Throughput-efficient sequential channel sensing and probing in cognitive radio networks under sensing errors. In *Proceedings of the 15th annual international conference on Mobile computing and networking* (2009), ACM, pp. 37–48.

[80] Si, W., Selvakennedy, S., and Zomaya, A. Y. An overview of channel assignment methods for multi-radio multi-channel wireless mesh networks. *Journal of Parallel and Distributed Computing 70*, 5 (2010), 505–524.

[81] Subramanian, A. P., Gupta, H., Das, S. R., and Cao, J. Minimum interference channel assignment in multiradio wireless mesh networks. *IEEE TMC 7*, 12 (2008), 1459–1473.

[82] Tan, S.-S., Zheng, D., Zhang, J., and Zeidler, J. Distributed opportunistic scheduling for ad-hoc communications under delay constraints. In *Proceedings of the 29th conference on Information communications* (2010), IEEE Press, pp. 2874–2882.

[83] Tang, J., Xue, G., and Zhang, W. Interference-aware topology control and QoS routing in multi-channel wireless mesh networks. In *ACM MobiHoc* (2005).

[84] Tragos, E. Z., Zeadally, S., Fragkiadakis, A. G., and Siris, V. A. Spectrum assignment in cognitive radio networks: A comprehensive survey. *IEEE Communications Surveys and Tutorials 15*, 3 (2013), 1108–1135.

[85] Viswanath, P., Tse, D. N. C., and Laroia, R. Opportunistic beamforming using dumb antennas. *Information Theory, IEEE Transactions on 48*, 6 (2002), 1277–1294.

[86] Wang, B., Wu, Y., and Liu, K. Game theory for cognitive radio networks: An overview. *Computer Networks 54*, 14 (2010), 2537–2561.

[87] Wu, H., Yang, F., Tan, K., Chen, J., Zhang, Q., and Zhang, Z. Distributed channel assignment and routing in multiradio multichannel multihop wireless networks. *Selected Areas in Communications, IEEE Journal on 24*, 11 (2006), 1972–1983.

[88] Wu, X., Liu, J., and Chen, G. Analysis of bottleneck delay and throughput in wireless mesh networks. In *IEEE MASS* (2006).

[89] Yu, S., Doss, R., Thapngam, T., and Qian, D. A transformation model for heterogeneous servers. In *High Performance Computing and Communications, 2008. HPCC'08. 10th IEEE International Conference on* (2008), IEEE, pp. 665–671.

[90] Yuan, J., Li, Z., Yu, W., and Li, B. A cross-layer optimization framework for multihop multicast in wireless mesh networks. *IEEE JSAC 24*, 11 (2006), 2092–2103.

[91] Zhang, H., Berg, A., Maire, M., and Malik, J. Svm-knn: Discriminative nearest neighbor classification for visual category recognition. In *Computer Vision and Pattern Recognition, 2006 IEEE Computer Society Conference on* (2006), vol. 2, pp. 2126–2136.

[92] Zhu, Y., Xu, B., Shi, X., and Wang, Y. A survey of social-based routing in delay tolerant networks: positive and negative social effects. *Communications Surveys & Tutorials, IEEE 15*, 1 (2013), 387–401.